

Timing and dynamics of the last deglaciation from European and North African $\delta^{13}\text{C}$ stalagmite profiles—comparison with Chinese and South Hemisphere stalagmites

D. Genty^{a,b,*}, D. Blamart^a, B. Ghaleb^b, V. Plagnes^c, Ch. Causse^d, M. Bakalowicz^e, K. Zouari^f, N. Chkir^f, J. Hellstrom^g, K. Wainer^{a,b}, F. Bourges^h

^aLSCE, UMR CEA/CNRS 1572, L'Orme des Merisiers CEA Saclay, 91191 Gif/Yvette cedex, France

^bGEOTOP, Université du Québec à Montréal, C.P. 8888, succ. Centre-Ville, H3C 3P8, Montréal, Canada

^cUMR Sisyphe 7619, Université Pierre et Marie Curie, cc123, 75252 Paris Cedex, France

^dCNRS Laboratoire de Moulis, 09200 Saint-Girons, France

^eISTEEM, Hydrosiences, CNRS-UMII, CC MSE, 34095 Montpellier Cedex 5, France

^fLRAE ENIS, Route de Soukra, BP W, 3038 Sfax, Tunisie

^gThe School of Earth Sciences, The University of Melbourne, VIC 3010 Australia

^hGéologie-Environnement-Conseil, F-09200 Saint-Girons, France

Received 1 May 2005; accepted 31 January 2006

Abstract

The last deglaciation and its climatic events, such as the Bølling–Allerød (BA) and the Younger–Dryas (YD), have been clearly recorded in the $\delta^{13}\text{C}$ profiles of three stalagmites from caves from Southern France to Northern Tunisia. The three $\delta^{13}\text{C}$ records, dated by thermal ionization mass spectrometric uranium–thorium method (TIMS), show great synchronicity and similarity in shape with the Chinese cave $\delta^{18}\text{O}$ records and with the marine tropical records, leading to the hypothesis of an in-phase (between 15.5 and 16 ka $\sim \pm 0.5$ ka) postglacial warming in the Northern Hemisphere, up to at least 45°N. The BA transition appears more gradual in the speleothem records than in the Greenland records and the Allerød seems warmer than the Bølling, showing here close similarities with other marine and continental archives. A North–South gradient is observed in the BA trend: it cools in Greenland and warms in our speleothem records. Several climatic events are clearly recognizable: a cooler period at about 14 ka (Older Dryas (OD)); the Intra-Allerød Cold Period at about ~ 13.3 ka; the YD cooling onset between 12.7 and 12.9 ± 0.3 ka. Similar to the BA, the YD displays a gradual climate amelioration just after its onset at 12.75 ± 0.25 ka, up to the Preboreal, and is punctuated by a short climatic event at 12.15 ka. Even though the Southern Hemisphere stalagmite records seem to indicate that the postglacial warming started about ~ 3 ka ± 1.8 ka earlier in New Zealand ($\sim 41^\circ\text{S}$), and about ~ 1 to ~ 2 ka earlier in South Africa (24.1°S), large age uncertainties, essentially due to slow growth rates, make the comparison still perilous. The overall $\delta^{13}\text{C}$ speleothem record seems to follow a baseline temperature increase controlled by the increase in insolation and punctuated by cold events possibly due to the N-America freshwater lake discharges.

© 2006 Elsevier Ltd. All rights reserved.

1. Introduction

The last deglaciation is punctuated by several climate events (i.e. transitions toward warm periods like the Bølling–Allerød or abrupt cooling such as the OD and YD), whose timing, amplitude, and distribution on the Earth are of primary importance if we want to understand their causes. It is certainly the best documented period of major climatic changes due to high resolution records from the ice core records (Alley et al., 1993; Dansgaard et al.,

*Corresponding author.

E-mail addresses: Dominique.Genty@cea.fr (D. Genty), ghaleb.bassam@uqam.ca (B. Ghaleb), Valerie.Plagnes@ccr.jussieu.fr (V. Plagnes), c.causse@free.fr (C. Causse), Michel.Bakalowicz@msem.univ-montp2.fr (M. Bakalowicz), Kamel.Zouari@enis.rnu.tn (K. Zouari), j.hellstrom@unimelb.edu.au (J. Hellstrom).

1993; Thompson et al., 1995; NorthGRIPmembers, 2004; EPICA, 2004), the ocean core records (Flower et al., 2004; Hendy et al., 2002; Hughen et al., 1995; Waelbroeck et al., 2001), the continental marine records (Turon et al., 2003) and the lake records (Allen et al., 1999; Grafenstein Von et al., 1999; Magri and Sadori, 1999; Stager et al., 2002; Zolitschka, 1992). Despite all these, there are still some uncertainties about the exact origin of the climate events of this period (i.e. the abrupt YD onset, the Older Dryas, the Inter Allerød Cold Period), the difference in the onset of deglaciation between the Northern and Southern Hemispheres, the occurrence and amplitude of the YD in the Southern Hemisphere, the climate variability during events such as the BA or the YD, etc. Difficulties in obtaining accurate absolute ages is certainly the main obstacle to resolving these questions: ^{14}C ages are complicated by the occurrences of ^{14}C plateaus during the deglaciation and by dead carbon fraction uncertainties; ice core layer counting appears difficult during cold and low accumulation periods like the YD; and finally, climatic signals are extremely various, from water stable isotopes to pollen in marine cores, that any comparison has to seriously consider the complexity of each proxy. It is likely that, depending on geographical location, latitude, and distance from the ocean, the deglaciation generated different imprints in palaeoclimatic records. Consequently, in order to get a better pattern of this period, the study of many geographically widespread records is necessary. Indeed, the goal behind an improved understanding of the BA/YD events is also to improve our understanding of the Dansgaard–Oeschger events that occurred during the last glacial period and whose origin might be similar (Blunier et al., 1998; Bond et al., 2001; Rahmstorf, 2003). In both cases, there are still questions about the origin of such sudden climatic shifts. Although the idea that large inputs of fresh water due to the melting of ice caps and discharge of water stored in huge North American lakes strongly reduced the North Atlantic ocean circulation is still the consensual hypothesis for events such as the YD, other hypotheses, involving a bipolar seesaw of a complex ocean-ice-atmosphere system (Blunier and Brook, 2001), stochastic resonance in an ocean-atmosphere climatic model (Ganopolski and Rahmstorf, 2002) or external forcing like solar activity variation are also evoked (Bond et al., 2001; Goslar et al., 1999; Hughen et al., 2000; Rahmstorf, 2002; Renssen et al., 2000; van Geel et al., 2003). The uncertainty in the causes is essentially due to the lack of accurate and absolute dated records, and to the uneven distribution of these records, especially on the continent (besides polar ice core archives), in the Southern Hemisphere and in low latitudes.

Well dated records of the last deglaciation on the European continent are rare, especially those whose dating is absolute thanks to annual layers counting or uranium–thorium dating and which possess a continuous record. Among them, there is the Lake Monticchio record where varve counting coupled with ^{14}C measurements on

organic matter allowed pollen–climate reconstructions of the last 102 ka (Allen et al., 1999). The last deglaciation and the YD are clearly recorded in this record, although with a low resolution due to pollen sampling constraints. Some stalagmites from Germany and Austria have partly recorded the last deglaciation period, but there was either a hiatus during the glacial-interglacial transition (Sauerland caves, western Germany) (Niggemann et al., 2003), or low resolution which prevented a good time constraint through this period (Hölloch Cave stalagmite where the Younger-Dryas and the Bölling Allerød occupy a few millimeters and where only two U/Th dated points could be made; (Wurth et al., 2004). The continuous Soreq Cave record (Israel) has brought precious information about the millennial scale climatic variation of the last 250 ka, as well as the Sapropel events linked to changes in the humidity and temperature of the Mediterranean Sea; the last deglaciation period was also recorded here in a composite record but the resolution for this particular period needs to be improved (Bar-Matthews et al., 2000; Bar-Matthews et al., 1999, 2003b). A very recent study shows that the last deglaciation was recorded in a 16.5 ka continuous stable isotopic record of a stalagmite from the Savi Cave (South-Eastern Alps of Italy) (Frisia et al., 2005). But here too, the transition from glacial to the beginning of the warming is not recorded and the transitions to the BA and to the YD are not clear because of a very slow growth rate during this period and very few U–Th ages (no age between 13.5 and 10.7 ka).

Outside of Europe there are also few speleothem records that cover the last deglaciation or a part of it: a stalagmite from the Onondaga Cave (Missouri, US) recorded a part of the Allerød–YD period in its stable isotopic profiles. Its very short growing period, about 0.8 ka long, and the uncertainties in the chronology do not allow any solid comparison with other records (Denniston et al., 2001). Chinese caves have recently brought well U/Th dated speleothem records: Hulu Cave (or Tangshan Cave) in East China and Dongge Cave in South China which both show striking similarities with the Greenland ice core records (Dykoski et al., 2005; Wang et al., 2001; Zhao et al., 2003). In the Southern Hemisphere, the New Zealand speleothems ($\sim 41^\circ\text{S}$) have recorded the last deglaciation linked with changes in the convergence of subtropical and sub-Antarctic waters (Hellstrom and McCulloch, 2000; Hellstrom et al., 1998; Williams et al., 2004). South Africa speleothem records also display a clear pattern of the last deglaciation in an area where other palaeoclimate proxies are very rare; they have shown that the temperature changed by about 6°C during this period (Holmgren et al., 2003; Talma and Vogel, 1992). From the above examples, it appears that speleothems can unravel the timing and the climatic structure of the last deglaciation in specific areas and thus help to better understand them: the chronology that relies on the U–Th analyses avoids the problems inherent to the ^{14}C dating methods and the climatic signal extracted from the calcite stable isotopes is relatively well

understood. But, up to now, there have been no such speleothem records in Europe that allow to decipher climatic events in the BA or YD periods, the timing of the beginning of the warming following the pleniglacial. The results we present in this study show a continuous speleothem record of the last deglaciation, and of the associated events such as the YD and the BA) on a NW-SE transect, in three different sites (Fig. 1): Villars Cave (SW-France, 45.30°N, 0.50°E, 175 m asl; Vil-stm11 stalagmite), Chauvet Cave (S-France, 44.23°N; 4.26°E; 240 m asl; Chau-stm6 stalagmite) and La Mine Cave (Central Tunisia, 35°N, 9.5°E, 1000 m asl; Min-stm1 stalagmite) (Fig. 1). The chronology was constructed through 29 thermal ionisation mass spectrometric uranium-thorium datings and climatic variations were characterized by 418 $\delta^{13}\text{C}$ and $\delta^{18}\text{O}$ measurements made along the growth axis of the stalagmites. All these sites are situated relatively close to the North Atlantic basin and thus have likely been influenced by any changes in this key area (i.e. ocean circulation, ice-sheet flooding dynamics, ocean–atmosphere interactions). The novelty of this study is also the use of the calcite $\delta^{13}\text{C}$ instead of the calcite $\delta^{18}\text{O}$ as a palaeoclimatic signal, which here appears much less variable from one site to another and also much more coherent when compared with the other records.

2. Site and sample descriptions

2.1. Villars Cave (45.30°N, 0.50°E, 175 m asl)

Villars Cave is located in a low porous Bajocian limestone at a depth of between 10 and 40 m. It is formed by a complex network of small galleries (1–3 m large) with some rare decametric chambers; the whole length of the cave is about 10 km and there are now only 2 small natural

entrances, far from each other, which explains why there is no noticeable air movement in the cave. Only during very cold periods can one occasionally observe a slight vapour plume at the small upper entrance. The present day vegetation above the cave consists of a deciduous forest of oak and hornbeam and the soil is between 0 and 20 cm thick, typical of an oceanic climate with mild winters (snow is rare) and relatively humid summers. Since 1993, the Villars Cave has been monitored for the hydrology (drip rate under stalactites; rainfall), temperature, air pressure and other environmental factors with automatic stations. Monthly seepage sampling, for the stable isotopes and geochemistry analyses, has also been done since this date, as well as modern calcite deposition experiments (Baker et al., 1998; Genty et al., 2001b). Averaged temperature in the upper galleries is $12.3 \pm 0.2^\circ\text{C}$, and $11.3 \pm 0.1^\circ\text{C}$ deeper in the cave. This difference might be due to the different orientation of the hill flanks that receive the rainfall feeding the stalagmites. Mean annual temperature from the nearby meteorological station (Nontron, 15 km far) is $12.2 \pm 0.7^\circ\text{C}$ (15 years) which is close to the upper galleries cave temperature (Table 1). While the annual cave temperature is very stable, there is a high seasonality in the outside air temperature with a mean summer (months JAS) temperature of $18.7 \pm 1.2^\circ\text{C}$ and a mean winter (JFM) temperature of $6.8 \pm 1.1^\circ\text{C}$. Mean annual rainfall is 1031 mm and it may vary by >500 mm from year to year. Note that the rainfall is distributed throughout the year (Fig. 2a). As a consequence, it is the seasonal temperature variations that control the water balance: the evapotranspiration is high in summer months leading to a negative theoretical water excess (rainfall minus evapotranspiration from the Thornthwaite calculation; Baker et al., 2000 and Fig. 2a) between about May and October. Water excess is positive in Villars from November to about April, which should

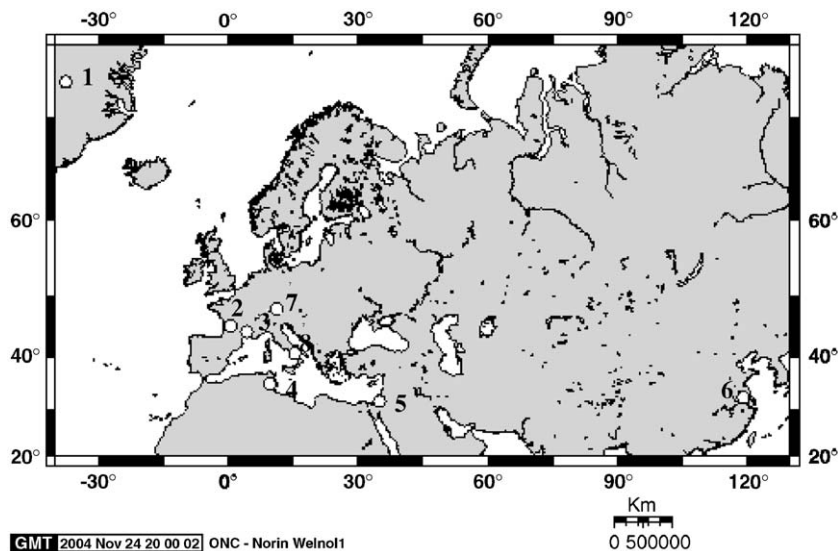


Fig. 1. Sites studied: 2 = Villars Cave (45.30°N, 0.50°E); 3 = Chauvet Cave (44.23°N, 4.26°E); 4 = La Mine Cave (35°N, 9.5°E). 1 = GRIP and GISP2 ice cores; 5 = Soreq Cave, Israel (Bar-Matthews et al., 2003b); 6 = Hulu Cave, China (Wang et al., 2001); 7 = Ammersee Lake, Germany (Grafenstein Von et al., 1999); 8 = Monticchio Lake, Italy (Allen et al., 1999).

Table 1
Meteorological settings of the studied sites (see Fig. 2 legend)

Cave	$R_{\text{ann. sep} \rightarrow \text{aug.}}$ (mm)	$R_{\text{nov.} \rightarrow \text{apr.}}$ (mm)	$R_{\text{may.} \rightarrow \text{oct.}}$ (mm)	$T_{\text{ann. sep} \rightarrow \text{aug.}}$ (°C)	Winter Tjfm (°C)	Sum. T jas (°C)	ETP _{ann.} (mm)	WE _{ann. > 0} (mm)
Villars 45.44 °N, 0.78 °E (Nontron, 1984 → 2004)	1031 (194)	586 (181)	102 (5)	12.2 (0.7)	6.8 (1.1)	18.7 (1.2)	720 (38)	535 (197)
Chauvet 44.23 °N, 4.26 °E (Orgnac, 1999 → 2001)	849	527	555	13.2	7.2	21.2	764	397
La Mine (Tunisia) 36.03 °N, 9.68 °E (Kairouan)	306	150	84	19.5	12.8	26.6	975	17

ETP = evapotranspiration deduced from the Thornthwaite formula (Thornthwaite, 1954). The annual water excess is the sum of the monthly water excess that is positive. Numbers in brackets indicate 1 sigma interannual variability for Villars where we have enough yearly data.

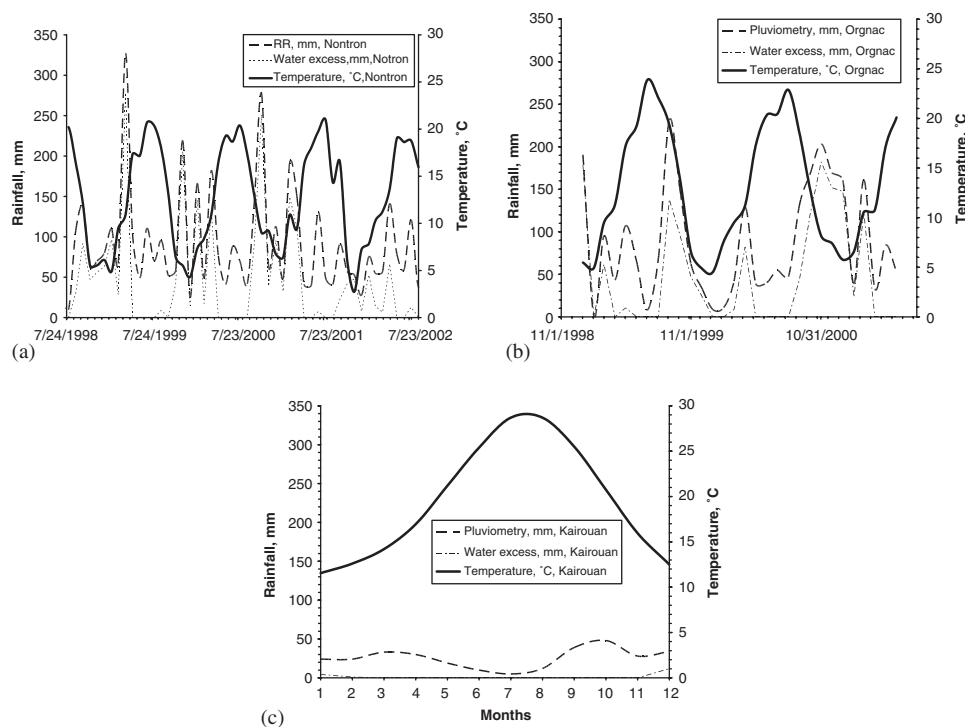


Fig. 2. Meteorological records from the closest meteorological stations from the caves studied : Nontron \approx 15 km from Villars Cave, Orgnac \approx 15 km from Chauvet Cave and Kairouan \approx 25 km from La Mine Cave. The water excess is the rainfall minus the evapotranspiration deduced from the Thornthwaite formula (Thornthwaite, 1954); it corresponds to the theoretical quantity of water that infiltrates in a karstic terrain.

correspond to the period when the karst recharge occurs. Monitoring in the Villars Cave for about 10 years had shown that the drip rate in the cave displays a seasonal behaviour, with an abrupt increase in November, which coincides with the beginning of the recharge. However, first results of stable isotope monitoring of the seepage water and of the rainfall at Villars indicates that the dripping water feeding the stalagmite ($-6.33\% \pm 0.18$ (1σ), $n = 93$; Table 2) is very close to the annual rainfall $\delta^{18}\text{O}$ weighted by the quantity of rain during the entire year ($-6.2\% \pm 0.5$ (1σ), from 1997 to 2002 AD; Fig. 3) and not only by the quantity of rain when the water balance is in excess (positive water excess, between November and April, which

is theoretically the water that infiltrates). This result would signify that the summer rains also participate in the seepage water $\delta^{18}\text{O}$ signal, which is usual in karstic terrains where the runoff is very limited and microfissures of the host rock allow rapid infiltration.

The Vil-stm11 stalagmite (Fig. 4) was found more than 200 m from the entrance, in the deep part of the cave about 40 m below the surface. It is 23.3 cm long and is essentially made of columnar calcite crystals that are coalescent (Kendall and Broughton, 1978), which makes the polished section appear dark and compact (Genty et al., 1997). The first 3 cm show an opalescent calcite (compact and “milky”) that coincides with the first stages of the growth

Table 2
Isotope composition of the seepage water (sw) and of the rainfall (r) of the three studied sites

Cave	$\delta^{18}\text{O}_{\text{sw}}$	δD_{sw}	$\delta^{18}\text{O}_r$	δD_r
Villars (Le Mas)	-6.3 ($n = 93$)	-38.3 ($n = 93$)	-6.2 (1997→2002)	-32.5 (1997→2002)
Chauvet (Orgnac)	-6.8 ($n = 27$)	-42.3 ($n = 27$)	-6.5 (2000→2001)	-40.9 (2000→2001)
La Mine (Tunis/Sfax)	-6.2 ($n = 1$)	-32.8 ($n = 1$)	-6.7 ^a (1992–2001, IAEA)	-39.7 ^a (1992–2001, IAEA)

All the data have been weighted by the rainfall and come from in situ or nearby monitoring except for the rainfall above La Mine Cave where we used the IAEA data of Tunis and Sfax corrected by an altitudinal gradient of $-0.3\text{‰}/100\text{ m}$.

^aThe rainfall isotopic composition of the La Mine site is not accurate due to the interpolation between two stations of Tunis and Sfax and also because of the altitudinal correction.

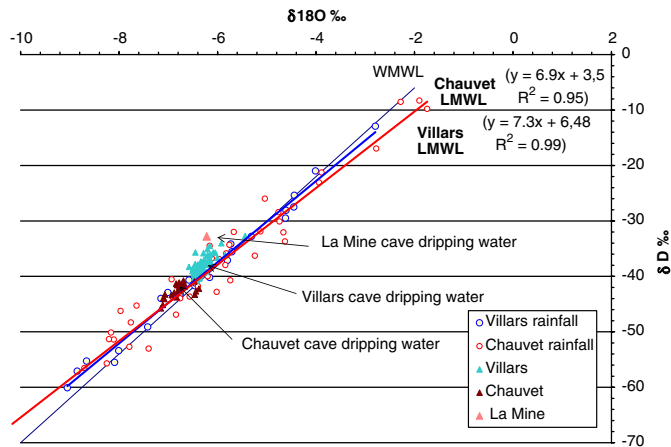


Fig. 3. Isotopic composition of the seepage water and of the rainfall at the three sites studied.

between 16 and 14 ka. We already observed such a fabric on the coldest periods in other stalagmites from the Villars Cave, just before their natural stop around 30 ka ago (Genty et al., 2003); it is certainly linked with specific environmental conditions but still not yet well understood. Four visible discontinuities made of infra-millimetric detrital layers occur at 7.1, 10.6, 20 and 21.9 cm from the base.

2.2. Chauvet Cave ($L = 44.23^\circ\text{N}$; $l = 4.26^\circ\text{E}$; 240 m asl)

Chauvet Cave, more than 200 m long, overlooks the Ardèche River canyon at a height of about 100 m. Its galleries developed in lower Cretaceous limestone whose permeability, like for Villars Cave, is mainly due to the microfissure network. There is more than 50 m of limestone above the ceiling of the cave, which explains the 2- to 4-day lag between any strong rainfalls and flooding in some parts of the cave. Chauvet Cave consists of a succession of very large chambers ($> 50\text{ m}$) whose present day entrance is a small passage (originally less than 1 m). The latter opens at the base of the limestone cliff and arrives at the ceiling of a large chamber, about 10 m in height. But the original entrance, about 10 m below, was certainly larger in order to allow the passage of cave bears and prehistoric humans for millenia; it collapsed, probably abruptly, between about 26 ka and 11.5 ka (Delannoy et al., 2001; Genty et al.,

2004b). Present day ventilation in the cave is poor and the CO_2 concentration high (Bourges et al., 2001). Its recent discovery, in December 1994 (Chauvet et al., 1995), was a revolution for prehistoric art history, especially because of its very old (i.e. $> 30\text{ ka}$) and elaborate paintings (Clottes et al., 1995; Valladas et al., 2001). The surface above the cave is covered by a typical Mediterranean vegetation composed of small bushes and sparse green oaks. As at the Villars site, the soil is very thin (i.e. between 0 and 20 cm thick). The climatic condition above the Chauvet Cave is mainly due to Atlantic storm tracks, like for the Villars site, but it has some Mediterranean influences with slightly warmer temperatures and lower annual rainfall (Table 1). Mean cave temperature is $13.0 \pm 0.2^\circ\text{C}$, which is close to the annual outside temperature (13.2°C , Table 1). Average annual rainfall is 849 mm; it is very variable ($> \pm 100\text{ mm}$) from one year to the next and there is no marked humid season. The average seepage water $\delta^{18}\text{O}$ is $-6.84\text{‰} \pm 0.14$ (1σ), ($n = 27$) which is slightly lower than the weighted mean annual rainfall $\delta^{18}\text{O}$ at Orgnac (-6.5‰ for the year 2000–2001; Fig. 3), but because we have only two years of measurement, this difference might not be significant. Note that the seepage water $\delta^{18}\text{O}$ value is slightly lower than in Villars Cave, possibly because of the higher altitude and because of its more continental position (Fig. 3).

The Chau-stm6 stalagmite is 67.2 cm long and has no visible hiatuses. The calcite is made of typical coalescent columnar fabric crystals (dark and compact on the polished sections) in the first 15 cm and in the last 10 cm, while the rest of the sample is slightly porous (mostly small intercrystalline porosity with occasionally visible growth lamina). It is interesting to note that Chau-stm6 grew on the archaeological soil of Chauvet Cave where charcoal particles brought in by humans have been found. The U–Th age of the first layers of the Chau-stm6 stalagmite, dated by U–Th at $32870 \pm 625\text{ yr}$, confirmed the ancient age of the nearby charcoal particles dated by ^{14}C AMS at $30550 \pm 370\text{ yr BP}$ uncalibrated ^{14}C age; (Genty et al., 2004b).

2.3. La Mine Cave (36.03°N , 9.68°E , 975 m asl)

La Mine Cave is located in the North of Tunisia, in Aptian Cretaceous limestone. Its small entrance, which is in fact an abandoned mine, opens on the flank of a mountain whose peak is 1305 m high. The main chamber,

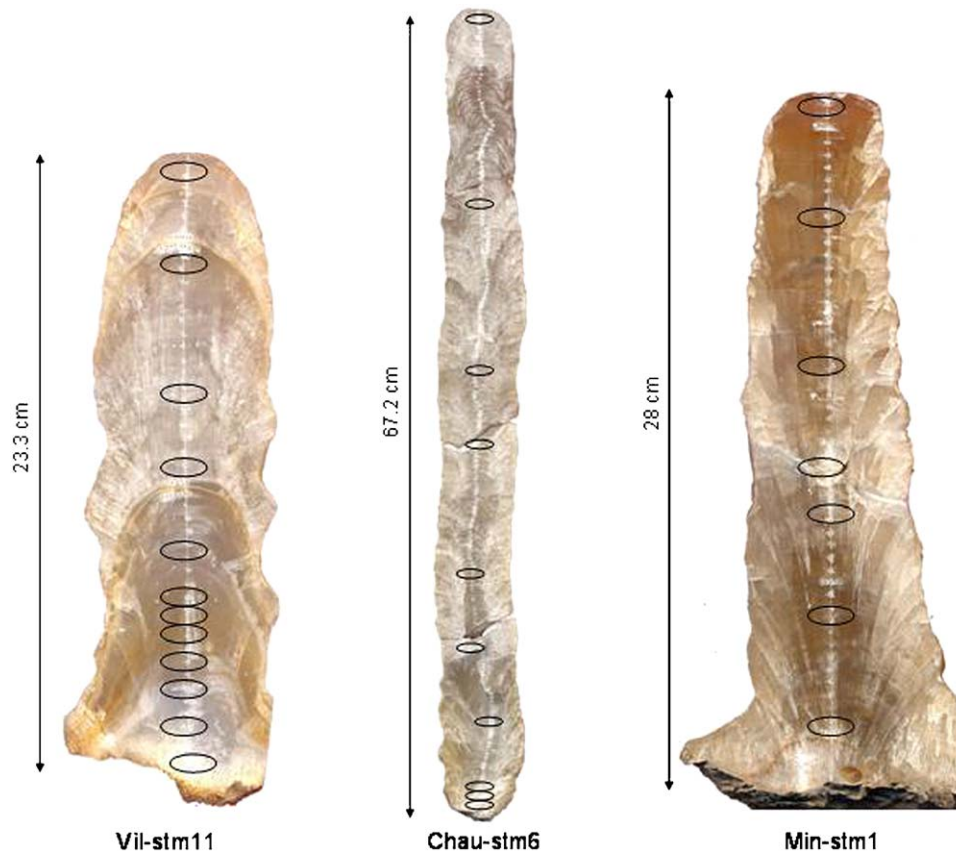


Fig. 4. Polished sections of the sample studied. Black circles indicate the U–Th samples.

where the stalagmite was sampled, is situated at the extremity of a narrow mine gallery about 250 m long, plunging 50 m deep. The mean annual rainfall at the nearby Kairouan meteorological station is 306 mm, which is significantly lower than at the two previous sites (Table 1) with a minimum during the summer (May → Sept.). Such a low rainfall associated with higher temperatures yields a very low water excess (Table 1). The average cave temperature is between 13 and 14 °C, which is much lower than the Kairouan average temperature (19.5 °C) because of the altitude. Winters are relatively mild with less than 10 days below freezing/year, which allows the growth of some green oak, Alep pine and Montpellier maple. Above the cave the soil is thin and the vegetation mostly composed of sparse trees and bushes. Most of the precipitation at this latitude in Northern Africa is linked with north-west winter storm track pathways and is not influenced by the monsoon (Gasse, 2000). The seepage isotopic composition made on only one sample (−6.2‰) appears higher than the rainfall composition (−6.7‰) (Table 2, Fig. 3). However the large uncertainties of the latter due to the interpolation between the Tunis and Sfax stations and to the altitude correction prevent any conclusion about a possible seasonal effect on the seepage water (i.e. more infiltration during winter).

Min-stm1 stalagmite was found in a large chamber (about 100 × 70 m), situated 50 m below the surface and

about 300 m from the entrance. Along its 28 cm height it is composed of a typical columnar fabric which appears very homogeneous, light brown in colour, compact and translucent on polished section (Fig. 4). Except at the very bases, no hiatus is visible on the stalagmite.

3. Methods

3.1. Stable isotope measurement

Samples were taken at the centre of the growth axis with a micro-drill (0.5 mm diameter). Calcite $\delta^{18}\text{O}$ was analysed with a VG OPTIMA mass spectrometer (LSCE, Gif-sur-Yvette) after orthophosphoric acid reaction at 90 °C. The data are expressed in the conventional delta notation relative to the V-PDB and the analytical error is $\pm 0.08\text{‰}$. In order to check the isotopic equilibrium of speleothems, we used the classical Hendy's test (Hendy, 1971) that should indicate the existence of kinetic fractionation due to evaporation or rapid CO_2 degassing: (1) a significant correlation between the $\delta^{18}\text{O}$ and the $\delta^{13}\text{C}$; (2) an enrichment in the $\delta^{13}\text{C}$ or $\delta^{18}\text{O}$ toward the edges of the stalagmite. We also tested the present day isotopic equilibrium by comparing the measured cave temperature with the theoretical equilibrium fractionation temperature estimated with the present day water and calcite $\delta^{18}\text{O}$ (O'Neil et al., 1969).

3.2. Uranium-series methods

The Vil-stm11 and Chau-stm6 were analysed at the GEOTOP (UQAM, B.G.). Samples were dissolved with nitric acid and spiked with a mixed ^{229}Th – ^{236}U – ^{233}U . Uranium and thorium fractions were separated on anion exchange columns using standard techniques (Edwards et al., 1987). Both uranium and thorium were loaded onto graphite-coated Re filaments and analyses carried out using a VG Sector mass spectrometer. The latter is equipped with an electro-static analyser and an ion-counting Daly detector. Errors were propagated from the in-run statistics and the uncertainties on the spike isotopic composition. Ages were calculated using the standard equation and the decay constants used for ^{234}U , ^{238}U , ^{230}Th and ^{232}Th were 2.835×10^{-6} , 1.55125×10^{-10} , 9.1952×10^{-6} and $4.9475 \times 10^{-11} \text{ yr}^{-1}$, respectively. The unusually low $^{234}\text{U}/^{238}\text{U}$ ratio of the Chau-stm6 sample (~ 0.55 instead of ~ 1) is due to a seepage water already depleted in ^{234}U as the $^{234}\text{U}/^{238}\text{U}$ of 0.8838 ± 0.0054 measured in the modern water of Chauvet Cave about 5 m from the stalagmite shows. This demonstrates that the local seepage water has passed through soil and rock in which the available uranium has been strongly depleted in ^{234}U due to preferential leaching and recoil effects over time.

The La Mine Cave stalagmite (Min-stm1) samples were analysed at the LSCE (Gif-sur-Yvette ; V.P., Ch.C.). Samples were combusted at 900°C for 1 h to oxidize the organic and mineral compounds of the speleothem matrix. Then, samples were dissolved by HCl (6N) in Teflon beakers containing a measured amount of mixed ^{233}U – ^{236}U – ^{229}Th spike. The sample-spike mixture (with carrier FeCl_3) was then left on a hot plate overnight to ensure complete ionic equilibration with the spike solution. Coprecipitation with NH_4OH (pH 7) separates U and Th from Ca. U and Th were separated using Dowex anion exchange resin conditioned with 6N HCl. U and Th were purified using Eichrom resins conditioned by 3N HNO_3 . U and Th fractions were loaded onto pre-outgassed single rhenium filaments with graphite coating and the isotope ratios were measured on a Finnigan Mat 262 mass spectrometer.

Detrital Th correction was performed on only two samples where the $^{230}\text{Th}/^{232}\text{Th}$ activity ratio is > 50 (two top samples of Vil-stm11; Table 1). The correction was undertaken with the hypothesis of an initial ratio $^{230}\text{Th}/^{232}\text{Th} = 1$ (Causse and Vincent, 1989). The detrital Th contamination for all the other samples is considered negligible (Table 1).

4. Results

4.1. Chronology and growth rate results

The chronology is secured by twenty nine ^{230}Th ages that were determined on the three stalagmites (Table 3; Fig. 5).

Average 2σ error on the final absolute age is 2%, with a maximum at 4.7% (basis of Chau-stm6) and a minimum at 0.7% (top of Min-stm1). The key factor is to estimate the age error of the climatic transitions that are located between any two dated points and whose timing is controlled by both the analytical errors and by the growth rate of the sample. Median growth curves and their associated 1- and 2-sigma uncertainty envelopes were constructed in two stages by following the method described in Drysdale et al (2004). Ages and uncertainties (including the effect of uncertainty of the initial $^{230}\text{Th}/^{232}\text{Th}$ value, which are significant for only the two top samples of Vil-stm11 stalagmite; Table 3) were calculated for each age determination using the Monte Carlo simulation in which those ages with overlapping uncertainties were constrained using a Bayesian approach (Ludwig, 2003). The outputs of the Monte Carlo simulation were then used to construct continuous curves using a repeated random walk, in which the growth rate between any two age determinations was allowed to vary randomly over one order of magnitude (2-sigma) for each iteration of the simulation. Note that should growth rate have varied over more than one order of magnitude between any two age determinations, then the true growth history for that interval might lie outside the curve depicted. For the beginning of the deglaciation (i.e. ~ 15 – 16 ka), average measured 2σ age error is from 175 to 350 yrs for Vil-stm11, from 130 to 400 yrs for Min-stm1 and from 255 to 460 yr for Chau-stm6. However, age errors at the base and near hiatuses of Vil-stm11, and for the first calcite layers of the Chau-stm6 stalagmite after the ~ 24 – 15 ka hiatus, are difficult to estimate because of the absence of continuous growth, and consequently of dated points exactly at the beginning of deposition. We did not use, therefore, the Monte Carlo simulation for these periods in the growth rate curves (Fig. 5). For the Min-stm1 sample, the slow growth rate of this period also explains the relatively high age error for the ~ 15 ka climatic transition. From growth rate curves (Fig. 5), the 2σ errors for this period can be reasonably estimated between 500 and 1000 yrs (Fig. 5b). Interpolated 2σ errors for the Younger–Dryas onset are slightly better: 600 yr (Vil-stm11), 500 yr (Min-stm1), 350 yr (Chau-stm6), all of which are still much higher than individual dating errors (Table 3; Fig. 5a). A decrease, or cessation of growth in the Vil-stm11 stalagmite during these periods prevented a good sampling resolution (made even more difficult by the low uranium content of the calcite, Table 1) which explains the relatively higher error for the YD period for this sample (Fig. 5b).

Among the four discontinuities observed on the Vil-stm11 stalagmite, one certainly corresponds to a deposition hiatus around ~ 9.3 ka (Fig. 5). As shown by the growth curve, another hiatus likely occurred during the Younger–Dryas or, at least, the growth rate was extremely low, but here there is no obvious visible discontinuity on the polished section. The three other discontinuities do not show any significant stop in the growth rate (checked

Table 3
Uranium–thorium ages

Sample	Position (mm/basis)	^{238}U (ppm)	$^{234}\text{U}/^{238}\text{U}$ activity	$^{230}\text{Th}/^{234}\text{U}$ activity	$^{230}\text{Th}/^{232}\text{Th}$ activity	\pm	U/Th age (years)	“+”	“−”	Age error (%)	Laboratory
Chau-stm6-U/Th-F	664	0.2848	0.00157	0.5700	0.00490	0.009910	0.00120	211	152	1.3	GEOTOP
Chau-stm6-U/Th-E	511	0.3286	0.00175	0.5544	0.00460	0.10590	0.00180	1119	230	1.9	GEOTOP
Chau-stm6-U/Th-D	3745	0.3102	0.00173	0.5592	0.00470	0.11490	0.00210	977	272	2.0	GEOTOP
Chau-stm6-U/Th-J	3245	0.3478	0.00221	0.5351	0.00740	0.11810	0.00190	644	252	1.8	GEOTOP
Chau-stm6-U/Th-B	2155	0.2565	0.00147	0.5816	0.00730	0.12370	0.00350	494	458	3.1	GEOTOP
Chau-stm6-U/Th-I	1525	0.3209	0.00176	0.5551	0.00650	0.127000	0.00190	626	254	1.7	GEOTOP
Chau-stm6-U/Th-H	92	0.5065	0.00266	0.5558	0.00609	0.20954	0.00368	134	574	2.2	GEOTOP
Chau-stm6-U/Th-A3	375	0.4408	0.00188	0.5415	0.00440	0.22694	0.00638	182	1011	3.4	GEOTOP
Chau-stm6-U/Th-A2	175	0.3772	0.00171	0.5646	0.00464	0.22627	0.00885	153	1370	4.7	GEOTOP
Chau-stm6-U/Th-A	10	0.4481	0.00219	0.5445	0.00435	0.25093	0.00370	82	619	1.9	GEOTOP
Min 1-U/Th-A	275	0.2583	0.005	1.3370	0.0070	0.0510	0.0010	441	37	0.7	LSCE
Min 1-U/Th-B	230	0.254	0.006	1.3217	0.0068	0.0717	0.0011	178	101	1.2	LSCE
Min 1-U/Th-C	175	0.2359	0.0061	1.3949	0.0075	0.0908	0.0012	755	110	1.1	LSCE
Min 1-U/Th-D	135	0.1650	0.0058	1.5024	0.0071	0.1036	0.0025	389	257	2.2	LSCE
Min 1-U/Th-E	115	0.1180	0.0063	1.4824	0.0078	0.1159	0.0037	478	401	3.0	LSCE
Min 1-U/Th-W	75	0.1404	0.0035	1.3825	0.0043	0.1443	0.0013	223	128	0.8	LSCE
Min 1-U/Th-X1	30	0.1200	0.0077	1.3602	0.0092	0.1891	0.0026	187	249	1.1	LSCE
VIL11-22,65	226.5	0.177	0.001	1.1894	0.0080	0.0559	0.0023	11	263	4.6	GEOTOP
VIL11-19,65	192.5	0.160	0.001	1.1969	0.0105	0.0639	0.0013	49	151	2.1	GEOTOP
VIL11-15	150	0.226	0.002	1.1954	0.0112	0.0759	0.0014	132	165	1.9	GEOTOP
VIL11-9,25	122.5	0.245	0.002	1.1918	0.0114	0.0770	0.0013	115	154	1.8	GEOTOP
VIL11-7,75	92.5	0.3062	0.00242	1.2067	0.0092	0.0877	0.0016	186	191	1.9	GEOTOP
VIL11-6,87	77.5	0.3487	0.00166	1.2162	0.00982	0.08760	0.00140	282	167	1.7	GEOTOP
VIL11-6,25	68.7	0.3871	0.00250	1.2320	0.01190	0.09060	0.00150	70	179	1.6	GEOTOP
VIL11-5,62	62.5	0.3574	0.00201	1.2289	0.00939	0.09830	0.00150	58	181	3.0	GEOTOP
VIL11-4,5	56.2	0.3415	0.00210	1.2298	0.01100	0.10850	0.00310	72	377	1.3	GEOTOP
VIL11-2,75	45	0.3573	0.00196	1.2313	0.01144	0.11588	0.00139	136	173	1.2	GEOTOP
VIL11-2,75	27.5	0.4907	0.00316	1.2258	0.12267	0.12267	0.00143	493	175	2.3	GEOTOP
VIL11-1	10	0.605	0.005	1.2285	0.0088	0.1316	0.0025	270	350	2.3	GEOTOP

Only the two samples which have a $^{230}\text{Th}/^{232}\text{Th}$ activity ratio less than 50 have been corrected for detrital Th (top of VIL11). The detrital calculation used corrects for both uranium and thorium detrital contribution to the sample. It is assumed that the detrital component has a $^{232}\text{Th}/^{238}\text{U}$ ratio of 1, that the detrital uranium is in secular equilibrium and that all the ^{232}Th is of detrital origin.

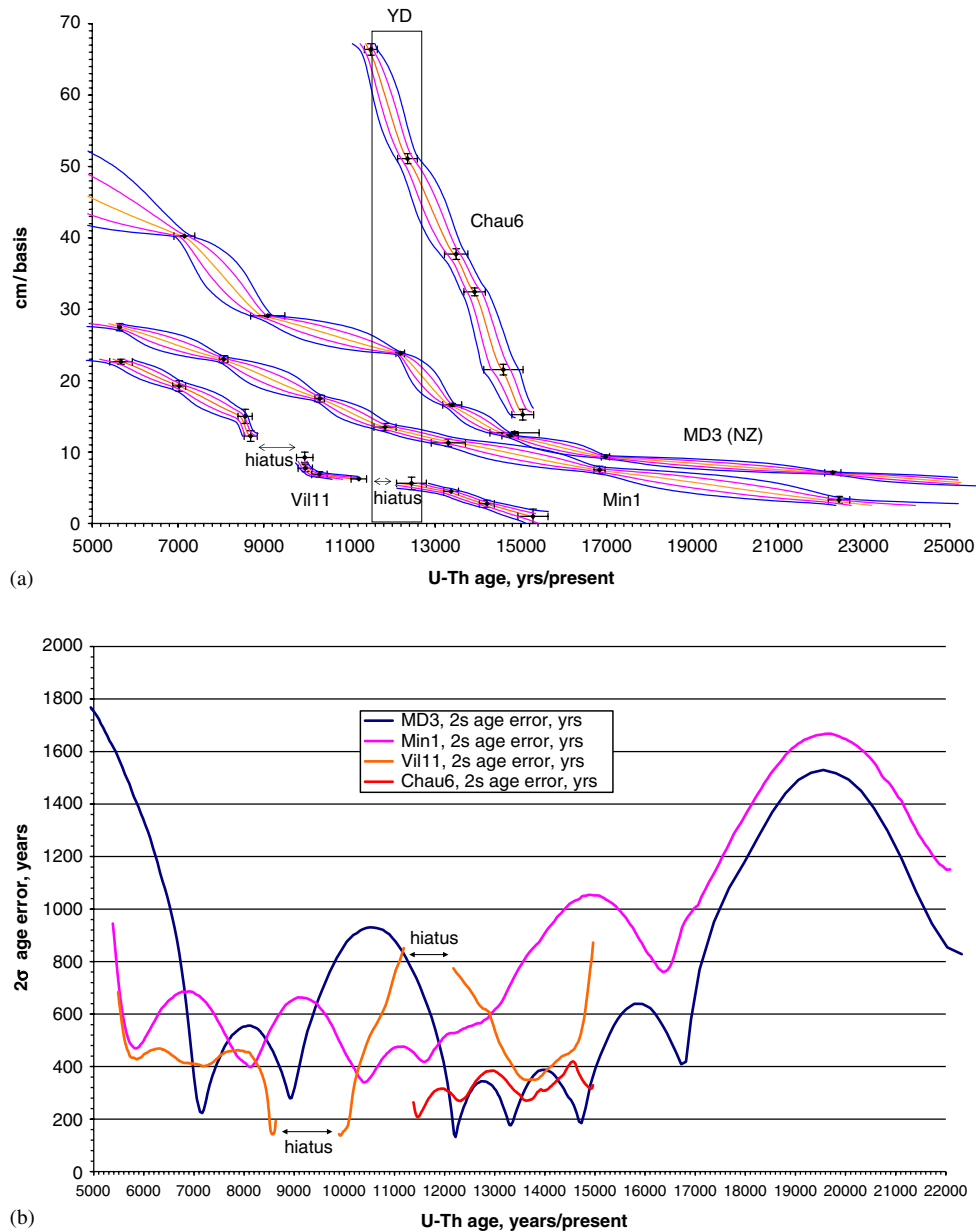


Fig. 5. (a) Growth rate curves of the Vil-stm11 (vill11; Villars Cave, SW-France), Min-stm1 (Min1; La Mine Cave, N-Tunisia), Chau-stm6 (Chau6; Chauvet Cave, S-France) and MD3 (New Zealand, (Hellstrom et al., 1998)). Point error bars are at 2σ blue lines are 2σ envelop, pink lines = 1σ envelop (see text for details). Note the high growth rate of the Chau-stm6 stalagmite even during the cold Younger–Dryas period, while it slowed down or stopped in the Villars stalagmite. (b) 2σ age uncertainty envelope taking into account isotope ratio measurement error, initial Th correction error, sample depth error and interpolation error (Drysdale, 2004; Ludwig, 2003).

thanks to AMS ^{14}C measurements) and are likely short local events that brought clay on the stalagmite surface. An interesting feature of this sample is that just after the ~ 9.3 ka hiatus, the calcite fabric is slightly more porous than below (brighter on the polished section because of the light reflection on crystal faces) and very regular lamina, about 0.8 mm thick, appear, testifying to a very fast growth rate during that period (~ 8.7 ka).

Mean vertical growth rate for the last 16 ka is much higher on the Chau-stm6 stalagmite (0.144 mm/yr) than for Vil-stm11 (0.022 mm/yr) and Min-stm1 (0.019 mm/yr) (Fig. 4). Note also the high growth rate of Chau-stm6

during the YD (~ 0.18 mm/yr; where it is contained within ~ 20 cm) while it is slowed to < 0.01 mm/yr in the Villars Cave stalagmite during this period, with possible hiatus(es) as suggested by a few brown layers observed on this sample. After 10 ka and until 8.5 ka, the Vil-stm11 growth rate increased to the very high rate of ~ 1 mm/yr, with visible growth lamina between 11 and 15 cm/base, which are about 1 mm thick (Fig. 5). The La Mine sample does not show a significant slowing in growth rate during the Younger–Dryas, but rather maintains a constant growth rate, suggesting that any climate change at this time did not affect the processes determining stalagmite growth.

4.2. Stable isotopic results

4.2.1. Isotopic equilibrium

For Vil-stm11 and the majority of Chau-stm6 stalagmites, the low correlation between $\delta^{13}\text{C}$ and $\delta^{18}\text{O}$ (along the growth axis or on single layers) and the absence of a significant trend toward the edge, suggest that isotopic equilibrium was reached during the calcite deposition of these two samples (Figs. 6,7). Only at 5 cm from the base does the Chau-stm6 sample display a significant enrichment in $\delta^{13}\text{C}$ that might be the consequence of a rapid degassing (Fig. 7). On the other hand, the significant correlation between $\delta^{13}\text{C}$ and $\delta^{18}\text{O}$ along the growth axis for the Min-stm1 suggests that kinetic effects might be important ($r^2 = 0.80$; $p < 0.01$; Fig. 6). However, measurements made along individual growth layers do not show any enrichment, suggesting that any ^{18}O and ^{13}C correlation is externally (climatically) driven and not a fractionation effect (Fig. 7). In all cases, the calculated temperature using equilibrium fractionation temperature estimated with the present day water and calcite $\delta^{18}\text{O}$ (O'Neil et al., 1969) is lower than or equal to that measured (Table 4). For the Chauvet and La Mine Caves the difference almost falls within the error margin but, in the Villars Cave, the difference is much more pronounced ($\sim 2^\circ\text{C}$), which suggests that the modern calcite $\delta^{18}\text{O}$ is about 0.5‰ higher than that which would have precipitated under isotopic equilibrium. This appears surprising because the lower galleries, where the modern calcite and the water come from, are probably among the most humid of the Villars Cave, as shown by the numerous pools and the absence of significant air flow. We would conclude that the isotopic equilibrium criteria, as defined by the classical Hendy tests,

are not entirely satisfactory: $\delta^{13}\text{C}$ and $\delta^{18}\text{O}$ correlate at least in one sample and most modern deposits are a little enriched in ^{18}O , as was observed in the first publications on speleothems (Fantidis and Ehhalt, 1970; Fornaca-Rinaldi et al., 1968). Anyway, despite these uncertainties concerning the isotopic equilibrium of both paleo and modern calcite deposits, we will see that an isotopic climatic signal is still preserved in all the stalagmites, especially in the $\delta^{13}\text{C}$ signal. One possible reason is that the kinetic fractionation due to an eventual evaporation or degassing effect would modify the $\delta^{13}\text{C}$ in the same direction as the climatic signal: for example, evaporation is likely to occur during dry and cold events, when the drip rate is lower, but during such climatic conditions, the vegetation and soil activity will slow, both phenomena leading to an increase in the calcite $\delta^{13}\text{C}$. Indeed, in such conditions, the $\delta^{13}\text{C}$ might also be enriched by prior calcite precipitation in the unsaturated zone (Baker et al., 1997). Replicate samples that cross cover a part of the record have been analysed from the Villars and Chauvet Caves (Fig. 8); no other samples were available from the La Mine Cave. They show that during the Holocene and the BA, both $\delta^{13}\text{C}$ and $\delta^{18}\text{O}$ signals are coherent: variations between contemporaneous samples that are within margins of modern sample variations and Holocene average values are very distinct than those from the BA. There is, however, a noticeable isotope event recorded on the Vil-stm6 sample, at the end of the Holocene, that was not recorded on the contemporaneous Vil-stm11 sample. This is possibly due to a local effect and time resolution differences.

Carbon isotope record—In all three samples, a large decrease is observed in $\delta^{13}\text{C}$ during the deglaciation period ($\approx 5\%$; Figs. 8a and 9, Table 5; note the inverted scale on

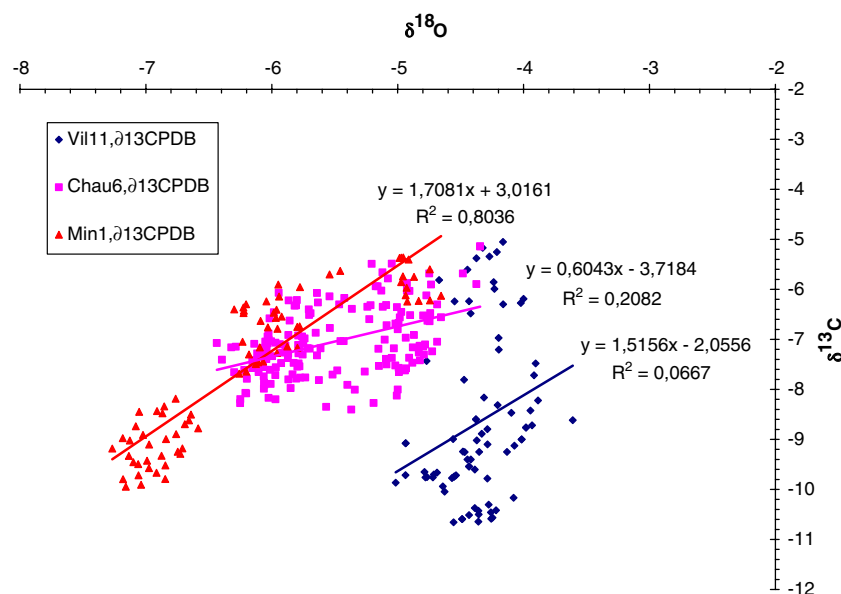


Fig. 6. Correlation between calcite $\delta^{13}\text{C}$ and calcite $\delta^{18}\text{O}$ for the three studied stalagmites. Note the significant correlation for the La Mine sample suggesting that a common factor, possibly kinetic fractionation, might have controlled both isotopes. However, double measurements made on single layers do not confirm this hypothesis.

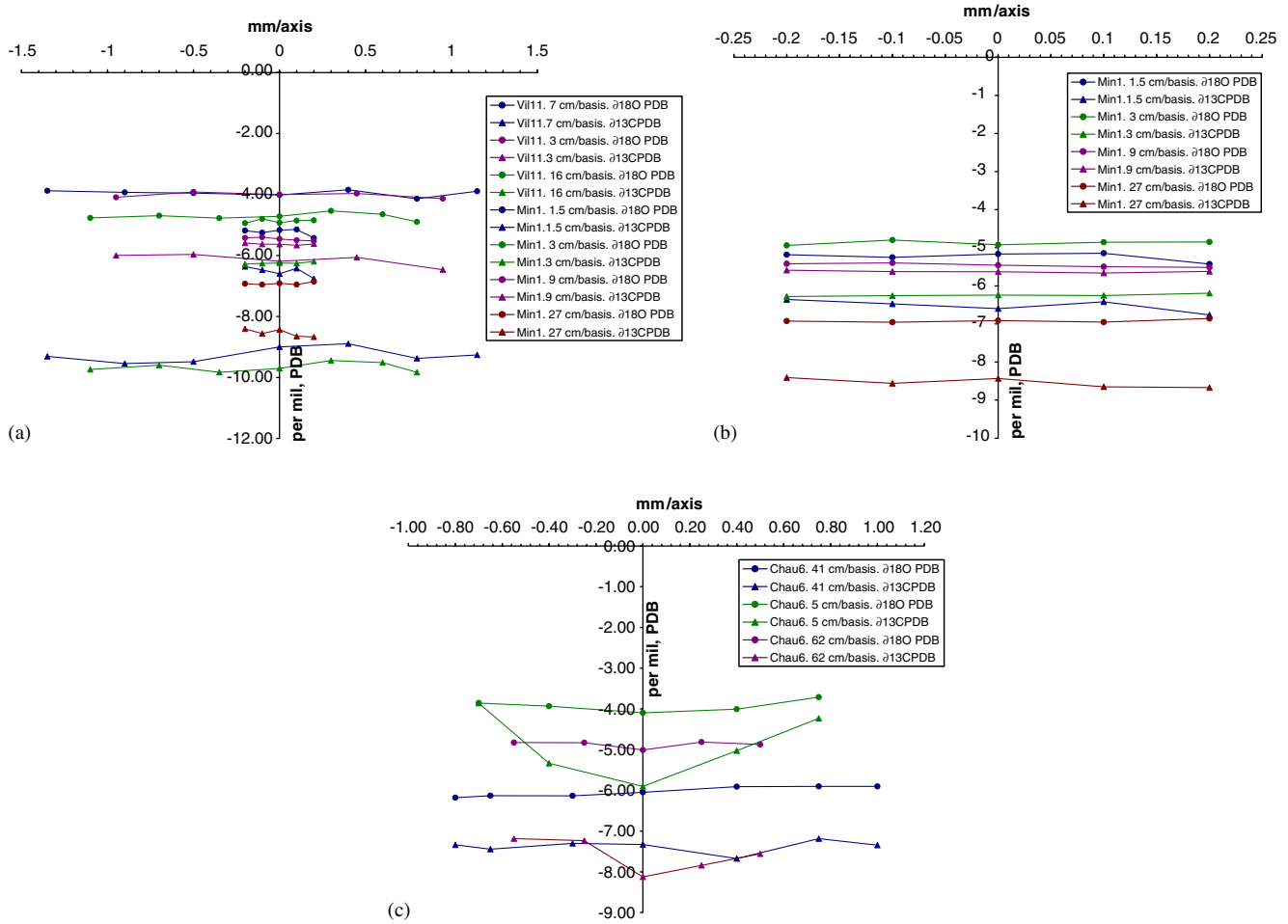


Fig. 7. Double isotope measurements on single layers on (a) Vil-stm11 (Villars Cave); (b) Min-stm1 (La Mine Cave); (c) Chau-stm6 (Chauvet Cave). Note that, except layer 5 on Chau-stm6, there is no significant isotopic trend toward the edges suggesting isotopic equilibrium everywhere.

Table 4
Present day equilibrium test (O'Neil, 1969)

Cave	Modern calcite $\delta^{18}\text{O}$, ‰ PDB ± 0.1	Modern water $\delta^{18}\text{O}$, ‰ VSMOW, ± 0.1	Measured temperature. ($^{\circ}\text{C}$), ± 0.1	Theoretical temperature. ($^{\circ}\text{C}$), ± 0.9
Villars (lower galleries)	−5.05 (top Vil#1A stalagmite)	−6.39 ($n = 45$)	11.3	8.95
Chauvet	−6.1 (top Chau4 and Chau1 stalagmites)	−6.81 ($n = 24$)	13.0	11.7
Chauvet	−5.34 (3 stalactites)	−6.81 ($n = 24$)	13.0	8.5
La Mine	−6.7 (top Min1 stalagmite)	−7.0 ($n = 2$)	13.5	13.5

Note that the Villars Cave theoretical temperature is significantly lower than the measured one suggesting that isotopic equilibrium is not reached today despite the high humidity of the cave and the distance of this measurement from the cave entrance. Note also that we have very few measurements for the La Mine Cave and that the equilibrium test must be taken with caution.

Y axis). The cold YD period is clearly visible on the Chauvet and La Mine samples with an abrupt $\delta^{13}\text{C}$ increase of 1.5‰ to 2.5‰ (Fig. 8a). It is less visible in the Villars sample, principally because of a very slow growth rate during this period which prevented a good temporal resolution (see growth curves, Fig. 5). In all samples, $\delta^{13}\text{C}$ displays a gradual decrease upon which smaller amplitude

events are visible (i.e. 1‰ amplitude) during the BA period (Fig. 8). An optimum is reached between 9.5 and 9.9 ka with the lowest $\delta^{13}\text{C}$ values on the Villars and La Mine stalagmites ($\delta^{13}\text{C} \approx -10$ to -10.5 ‰). It is followed by a slight $\delta^{13}\text{C}$ increase of about 1.5‰ until ~ 6 ka.

Oxygen isotope record—In contrast to the $\delta^{13}\text{C}$ signal, where there is a quite good agreement between stalagmite

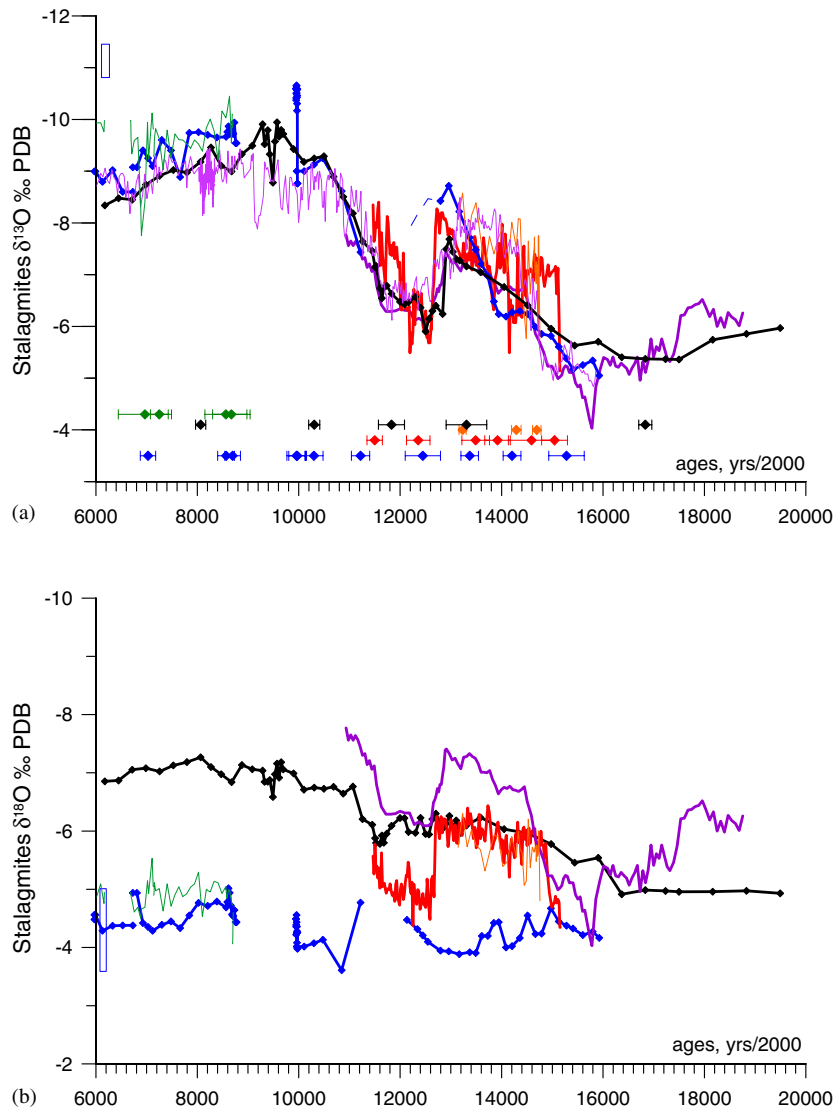


Fig. 8. $\delta^{13}\text{C}$ (a); and $\delta^{18}\text{O}$ (b) profiles of the three studied stalagmites : blue line = Vil-stm11 (Villars Cave, SW-France), red line = Chau-stm6 stalagmite (Chauvet Cave, S-France), black line = Min-stm1 stalagmite (La Mine Cave, Tunisia). The green (Vil-stm6) and orange (Chau-stm3) curves are two replicates from Villars and Chauvet caves respectively. Comparison with the $\delta^{18}\text{O}$ record of Hulu Cave (China), PD stalagmite dated by TIMS U–Th (violet line; Wang et al., 2001) and with the $\delta^{18}\text{O}$ record of Dongge Cave (China), D4 stalagmite (light violet line; Dykoski et al., 2005). Diamonds indicate TIMS U/Th dated points with 2σ error bars. Blue boxes at the left of the axis indicate present day values for the Villars Cave site. Note that the deglaciation and the YD are well marked on the $\delta^{13}\text{C}$ graph while less clear on the $\delta^{18}\text{O}$ one. Note also, that during the YD, the Villars Cave stalagmite slowed down drastically or stopped growing (see growth curve in Fig. 5).

isotope profiles, the calcite $\delta^{18}\text{O}$ records of our samples display significant differences between samples and also different features (Fig. 8; Table 5): (1) the deglaciation is not visible in the Villars stalagmite where the $\delta^{18}\text{O}$ remains relatively stable within a 1‰ variation; (2) the $\delta^{18}\text{O}$ does not clearly show the YD in the Villars and La Mine samples. However, the $\delta^{18}\text{O}$ record of the Chau-stm6 sample is very similar to the $\delta^{13}\text{C}$: it recorded the BA transition, the cold episode during the BA period and the YD. This raises the question of why the stalagmite $\delta^{13}\text{C}$ records climate change in all three stalagmites while the $\delta^{18}\text{O}$ displays a marked climatic signal only in the Chauvet Cave sample.

5. Discussion

5.1. Interpretation of the stable isotopic signals

5.1.1. Understanding the $\delta^{13}\text{C}$ signal

Carbon in speleothem calcite has two main sources: (1) soil CO_2 which is controlled by atmospheric CO_2 , plant respiration, and organic matter degradation; (2) bedrock carbonate (CaCO_3) that is dissolved during seepage. It has been demonstrated, by the detection of the ^{14}C bomb-peak (produced by nuclear tests in the atmosphere) on modern stalagmites, that in most temperate caves (among them Villars Cave) between 80 and 90% of the speleothem

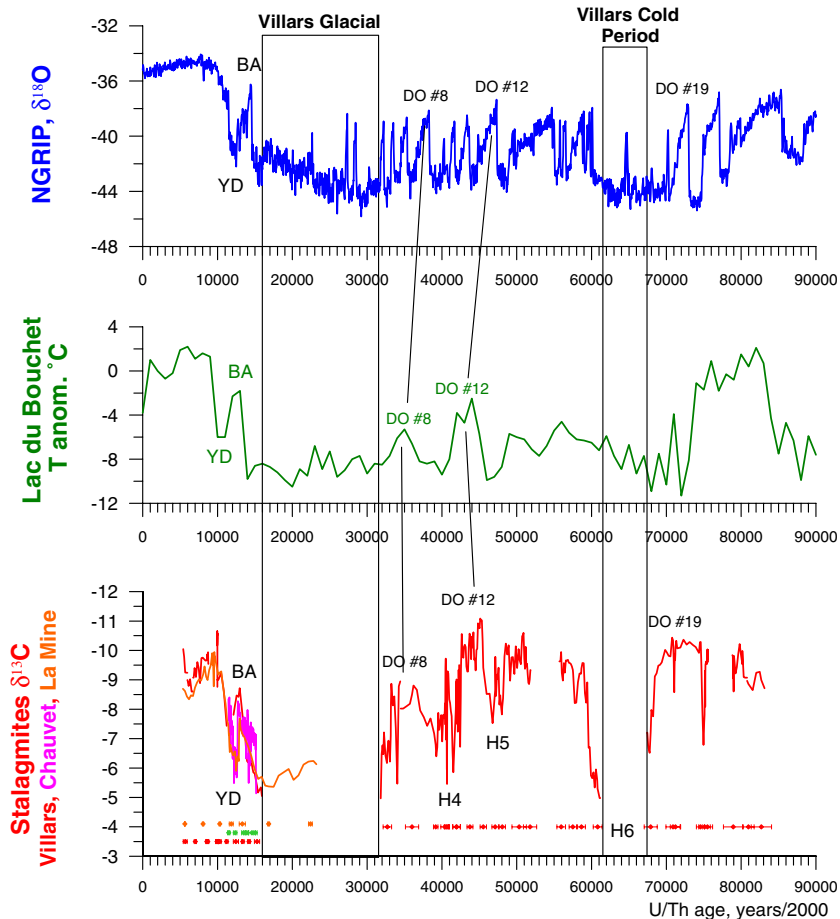


Fig. 9. Stalagmite $\delta^{13}\text{C}$ profile of the last 90 ka, from the caves of Villars (Dordogne, SW-France), Chauvet (Ardèche, S-France) and La Mine (N-Tunisia). Comparison with: Greenland ice core record of NGRIP (NorthGRIPmembers, 2004), temperature reconstruction from pollen assemblages of the Bouchet Lake (Beaulieu de and Reille, 1992; Guiot et al., 1993). “Villars Glacial” and “Villars Cold period” are hiatuses found in Villars Cave samples, due to extremely cold conditions that prevent seepage and calcite precipitation.

carbon comes from the soil CO_2 (Genty et al., 2001a; Genty and Massault, 1999; Vogel and Kronfeld, 1997). These studies also demonstrated that the carbon isotope (^{12}C , ^{13}C , ^{14}C) transfer from the atmosphere to the soil and to the stalagmite calcite is relatively quick (i.e. 5–15 years) leading to a rapid response in the $\delta^{13}\text{C}$ of modern calcite. The high proportion of soil CO_2 , can be explained by the fact that, during seepage, dissolution takes place in most cases under an “open system” where continuous exchanges occur between the gas, solid and liquid phases (Drake, 1983; Ford and Williams, 1992). For all these reasons, stalagmite $\delta^{13}\text{C}$ must be very sensitive to any changes in the soil (microbial activity) and vegetation (plant root respiration) above the cave. Some authors have interpreted the speleothem $\delta^{13}\text{C}$ signal as the result of changes in the vegetation types (C4/C3 plant ratio; Denniston et al., 2001; Dorale et al., 1998, 1992; Salomon and Mook, 1986), which is reasonable for specific areas but not in these sites. No evidence of C4 plants has been found during the last Glacial (Paquereau, 1980) in Southern-France and they are unlikely in Northern-Tunisia. The most likely explanation for the $\delta^{13}\text{C}$ variation is that previously suggested for the Dansgaard–Oeschger events recorded in a stalagmite from

the Villars Cave (Genty et al., 2003) and in a stalagmite from New Zealand where the last deglaciation was observed (Hellstrom et al., 1998): the $\delta^{13}\text{C}$ is mainly controlled by the soil biogenic production (plant root respiration and microbial activity of the soil and the epikarst zone), which is linked to climatic factors such as temperature and humidity. Consequently, a climate amelioration triggers the microbial activity in the soil above the cave allowing vegetation to develop, both phenomena producing a CO_2 depleted in ^{13}C and leading to a decrease in the speleothem $\delta^{13}\text{C}$. Conversely, a climate degradation like the one observed at the onset of the Younger–Dryas considerably reduced the plant and soil activity mainly because of the temperature decrease. As a consequence, the $\delta^{13}\text{C}$ of the dissolved CO_2 will be much less influenced by biogenic CO_2 and more by atmospheric CO_2 , leading to an increase in the speleothem $\delta^{13}\text{C}$. During extreme climatic events, when the climate becomes too cold and dry, the $\delta^{13}\text{C}$ increase is followed by a hiatus in the stalagmite: this is the case for the Villars sample which did not grow before $15925 \text{ yr} \pm 350 \text{ yr}$; and for the Chauvet sample that did not grow between $15160 \text{ yr} \pm 250 \text{ yr}$ and $24260 \text{ yr} \pm 570 \text{ yr}$ (Genty et al., 2004b). If the Southernmost sample,

Min-stm1 stalagmite, does not show a hiatus during the pleniglacial, it is likely because the climate of North Tunisia was less severe than in France, similar to the Soreq Cave records (Israel) where continuous growth occurred (Bar-Matthews and Ayalon, 2002; Bar-Matthews et al., 1997). In contrast, in stalagmite records to the north of those studied here, climate conditions were too severe for stalagmite growth and deposition before 10,000 yrs is rare (Baker et al., 1993).

The abruptness and synchronism of the $\delta^{13}\text{C}$ transitions seem to indicate that these changes happened quickly. Studies of the ^{14}C bomb-peak on modern stalagmites suggest that this is possible, without significant lag with climatic changes, highlighting a difference with pollen records where changes in taxa due to the plant colonization from refuges may have a significant inertia. The agreement between our $\delta^{13}\text{C}$ records is much more apparent when we compare our new deglaciation $\delta^{13}\text{C}$ records to the published last glacial $\delta^{13}\text{C}$ record of a Villars stalagmite (Fig. 9): the warm Dansgaard-Oeschger episodes are characterised by low $\delta^{13}\text{C}$ (−10.4‰, −11‰, −8.8‰ for the DO#19, #12, #8, respectively), whilst on the other hand, the $\delta^{13}\text{C}$ is quite high for the periods coinciding with the Heinrich events (−5.3‰, −7.5‰, −5.4‰ for the H6, H5 and H4, respectively; Fig. 9). As in the pleniglacial in the Villars and Chauvet samples, the extreme cold phase, between 67.4 and 61.2 ka, is marked by a hiatus coinciding with MIS 4 and the H6 event.

Even if we favour the biogenic control for the observed calcite $\delta^{13}\text{C}$ variations, other environmental factors might have been superposed and played a significant role: the effect of temperature on equilibrium fractionation processes, kinetic fractionation due to fast CO_2 degassing, prior calcite precipitation due to dry conditions and changes in atmospheric $\delta^{13}\text{C}$ and CO_2 concentration changes (Baker et al., 1997; Dulinski and Rozanski, 1990; Mickler et al., 2004). Among the different processes that might influence the $\delta^{13}\text{C}$ variations there is:

- (1) a slow soil–water residence time which will prevent complete soil CO_2 equilibration with the water due to the slow CO_2 hydration rate (Liu and Dreybrodt, 1997); as a consequence, a larger imprint of the atmospheric CO_2 will cause an enrichment of the carbon isotopic composition of the calcite. In that case, the high $\delta^{13}\text{C}$ of the calcite would be associated with humid periods, like observed for example in the Soreq and Peqiin Cave records for stage 5e (Bar-Matthews et al., 2003a). However, this process is not likely in our records because warmer and more humid periods (BA, Holocene) are associated with lower $\delta^{13}\text{C}$;
- (2) a kinetic effect due to fast CO_2 degassing: because the light carbon atoms escape more quickly than heavy carbon atoms precipitate (during the calcite precipitation), the remaining DIC $\delta^{13}\text{C}$ will increase and will produce an enrichment in the carbon isotopic signal. But this effect should be small because only about 10%

of the DIC is lost during degassing (Clark and Lauriol, 1992; Hendy, 1971); and

- (3) drier periods that will favour the prior calcite precipitation and consequently will enrich the calcite $\delta^{13}\text{C}$ (Baker et al., 1997); there is no argument against this phenomenon, since we do not yet have trace element analyses that would confirm or not the importance of this effect (Hellstrom and McCulloch, 2000).

Consequently, it is likely that processes 1 and 2 have little importance in our stalagmite $\delta^{13}\text{C}$ record. For the last process (3), its effect goes in the same direction as the climatic changes and, as explained before, will likely be superimposed on climatic effects. But more investigations appear necessary to determine their relative influence as stated by McDermott (McDermott, 2004).

5.1.2. Understanding the $\delta^{18}\text{O}$ signal

The calcite $\delta^{18}\text{O}$ value of a stalagmite is controlled by several factors that can act in opposite directions: (1) the isotopic equilibrium fractionation, which is controlled by cave temperature (usually assumed to be close to the mean annual external temperature, but as the cave temperature can vary significantly within a cave—i.e. there is a difference of 1.1 °C between low and high galleries in the Villars Cave—this assumption should be more frequently discussed in speleothem-based palaeoclimate studies) and whose value is about $-0.24\text{‰}/^\circ\text{C}$ (Kim and O’Neil, 1997; O’Neil et al., 1969); (2) the seepage water $\delta^{18}\text{O}$, which is similar to the average $\delta^{18}\text{O}$ of the rain above the cave and which depends on the cloud condensation temperature of the site studied; (3) changes in rainfall storm track pathways; and (4) variations in the ocean water $\delta^{18}\text{O}$, the main source of vapour. In Villars, there is a significant seasonal correlation ($R^2 = 0.41$) between the rainfall $\delta^{18}\text{O}$ and the air temperature of $+0.36\text{‰}/^\circ\text{C}$ (monthly monitoring since 1997). If this value is considered close to the inter-annual $\delta^{18}\text{O}/\text{T}$ gradient (which might have changed between the YD and the Holocene), then it will cancel at least in part the fractionation due to equilibrium calcite precipitation. This, and other complex interactions between changes in rainfall source and $\delta^{18}\text{O}$ changes, could explain why in the Villars stalagmite, the calcite $\delta^{18}\text{O}$ signal does not show clearly the last deglaciation temperature change. The difference in the average calcite $\delta^{18}\text{O}$ values between each sample is also due to their geographical location: Villars is closest to the ocean (less than 200 km) and at the lowest altitude (175 m asl), hence its average $\delta^{18}\text{O}$ for the Holocene part of the record (from ~10 to ~5 ka) is much more enriched compared to the more continental caves (mean Vil-stm11 $\delta^{18}\text{O}$ is -4.48‰ against -6.96‰ for the higher, 975 m asl, La Mine Cave stalagmite). The Chauvet Cave sample displays much more $\delta^{18}\text{O}$ variability, and despite the fact that it recorded all the climatic events much better than the two other stalagmites we can not explain this contrasting behaviour in a satisfactory manner. Meteorological and isotopic settings

are close to those of Villars Cave (Tables 1 and 2), the depth of the rock formation above the samples studied is also very similar. The differences between Chauvet and Villars may be due to the slightly more “continental” position of the Chauvet Cave where the seepage water and the rainfall isotopic composition are lower (Table 2) and possibly more sensitive to any change in the storm track pathways (Rozanski et al., 1993), but here too more measurements of rainfall and seepage cave isotopic composition are necessary to be affirmative.

5.2. Timing of the lateglacial warming and transition toward the Bolling–Allerod

The exact timing of the beginning of the post-glacial warming can not be accurately dated on the Vil-stm11 and Chau-stm6 samples because of the absence of deposition during the full glacial period, which makes it difficult to see the beginning of the transition. For the Min-stm1 sample, it is the slow growth rate during this period that prevents a small error in the age estimate (Fig. 5). However, both Vil-stm11 and Chau-stm6 samples started to grow synchronously, probably because in both cases the climate passed a threshold (temperature/humidity) allowing the growth of speleothems. Vil-stm11 started to grow at $15925 \pm \sim 500$ yr ago, as soon as the climate allowed water infiltration, soil CO_2 production and limestone dissolution (Figs. 5 and 8). Its $\delta^{13}\text{C}$ started to decrease at the same time, demonstrating that the biological activity of the soil and epikarst above the cave had begun. Synchronously within the 2σ error bars, the Chau-stm6 stalagmite started to grow at $15160 \pm \sim 500$ yrs, after a hiatus of about 8 ka (the base of this stalagmite grew between 34233 ± 625 and 24255 ± 550 yr). All other dated stalagmites in this cave grew after this cold period, i.e. < 16 ka (Genty et al., 2004a). Similar to the Villars stalagmite, the Chau-stm6 $\delta^{13}\text{C}$ started to decrease immediately after the commencement of growth, but the transition toward the Bolling is much more abrupt than in Villars and occurred in less than ~ 150 yr (interpolated value; Fig. 8). On the other hand, the Tunisian stalagmite (Min-stm1) displays a continuous record which started much earlier, at $23200 \pm \sim 500$ yr. This is likely due to the southernmost location of the La Mine Cave where the climate was not too cold or dry to prevent drip water seepage; this is similar to what is observed in the Soreq Cave record, which is at a slightly lower latitude. The Min-stm1 $\delta^{13}\text{C}$ started its decrease $16370 \pm \sim 780$ yr ago, which is synchronous with the Vil-stm11 stalagmite and slightly earlier than the Chau-stm6 one, but still within the 2σ error (Fig. 8).

Surprisingly, the shape of both the Hulu Cave (China, 32.3°N , Wang et al., 2001; also called the Tangshan Cave in Zhao et al., 2003) and of the Dongge Cave $\delta^{18}\text{O}$ records (China, 25.17°N , Dykoski et al., 2005), both several thousands km east and with a climate mainly influenced by the monsoon, can be superimposed almost perfectly on our $\delta^{13}\text{C}$ records (Fig. 8). The climate improvement,

marked by a decrease in $\delta^{18}\text{O}$, starts at the same time as in our samples: $15780 \pm \sim 200$ yr for the PD stalagmite, 16073 ± 60 yr for the YT stalagmite (Wang et al., 2001) (Fig. 8), and ~ 15 ka for the 996182 stalagmite which is less well time constrained (Zhao et al., 2003). Despite its extremely well constrained chronology, the beginning of the deglaciation is more difficult to see on the Dongge Cave stalagmite because it seems to coincide with the beginning of its growth, about ~ 16 ka ago (Dykoski et al., 2005). For these Chinese cave samples, the ratio of summer to winter precipitation is the main factor that controls the calcite $\delta^{18}\text{O}$; its decrease implies that a more intense East Asia Monsoon occurred, probably because of warmer temperatures. Because the Hulu Cave record is continuous over the last glacial period and recorded the entire climatic transition (see Wang et al., 2001), we are sure that these dates correspond to the first noticeable warming phase of the deglaciation.

At a more eastern location than Europe or Tunisia, and at a slightly lower latitude (31.6°N) than the La Mine Cave, the Soreq Cave speleothem $\delta^{18}\text{O}$ record, mainly controlled by the rainfall amount, also recorded not only the Sapropel events during the last glacial period, but also recorded the last deglaciation and the YD (Bar-Matthews et al., 2000, 2003b) (Fig. 10). Except for the early Holocene event, likely due to extremely high precipitation, the $\delta^{13}\text{C}$ record of Soreq Cave displays changes during the last deglaciation which are very similar to those found in our samples and in Hulu Cave: a gradual $\delta^{13}\text{C}$ decrease > -4 ‰ until the onset of the YD (Fig. 10). As in our records, the gradual $\delta^{13}\text{C}$ decrease observed at Soreq could be due to the development of soil activity and vegetation, linked to climate change as demonstrated by the synchronous $\delta^{18}\text{O}$ variations. However, the very beginning of the post glacial warming occurred much earlier in the Soreq Cave record, at $19 \pm \sim 0.5$ ka, and the most pronounced climatic change started at $\sim 16.7 \pm \sim 0.5$ ka, which is slightly earlier than in our records but still within errors. As we will see, the YD appears also about ~ 0.7 ka earlier compared to the other N-hemisphere records, but this might be due to limited U–Th dates around this period.

Comparison with Southern Hemisphere records shows that, from both isotope profiles (calcite $\delta^{13}\text{C}$ and $\delta^{18}\text{O}$), the first sign of warming (recommencement of surface biological activity) seems to have begun earlier in the Southern Hemisphere speleothems than in those from the Northern Hemisphere (except at Soreq) (Fig. 10): 19.0 ± 1.6 ka for the two high altitude cave samples (Hellstrom et al., 1998), and between 20 and 18 ka for the coastal stacked samples record (Williams et al., 2004). But, the main climatic change, as shown by more abrupt isotope changes (and especially in the $\delta^{13}\text{C}$ signal of the MD3 stalagmite; red line, Fig. 7c) occurred at $16.7 \pm \sim 0.45$ ka, which coincides with the rapid return to dense forest cover in this part of New Zealand, and which is slightly earlier to the 15.5–16 ka transition observed in our samples, but still within the 2σ error margin for the Min-stm1 stalagmite. Both New

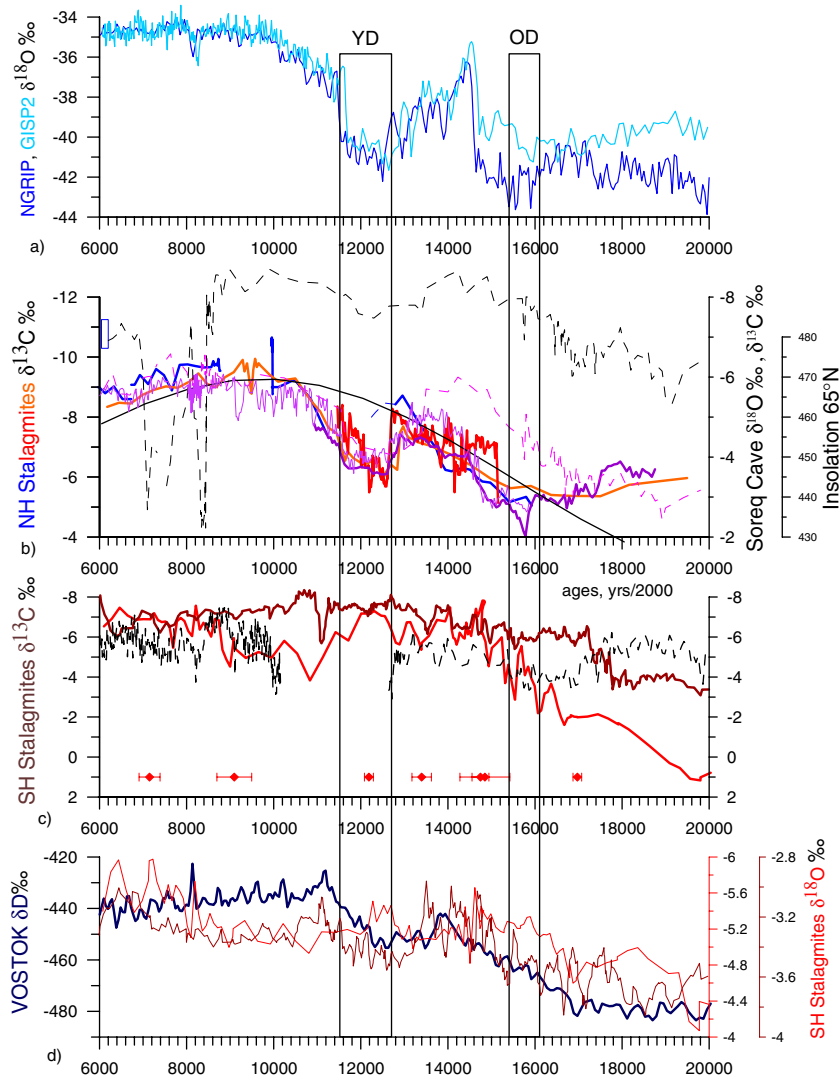


Fig. 10. Inter-hemispheric comparison of U–Th TIMS dated speleothem records, correlations with ice core records: (a) Greenland ice core records of NGRIP (NorthGRIPmembers, 2004) and GISP2 (Grootes et al., 1993). (b) Villars, Chauvet and La Mine $\delta^{13}\text{C}$ profiles (this study) with Soreq Cave speleothem records (black dashed lines = $\delta^{13}\text{C}$; pink = $\delta^{18}\text{O}$). Superimposed: 65°N insolation (Berger and Loutre, 1991) and Chinese stalagmites from Hulu Cave (violet; Wang et al., 2001) and from Dongge Cave (light violet line; Dykoski et al., 2005); (c) $\delta^{13}\text{C}$ records of Southern Hemisphere speleothems: red = MD3 stalagmite, Nettlebed Cave, dated points with 2σ errors at the bottom (New Zealand; Hellstrom and McCulloch, 2000; Hellstrom et al., 1998); brown = stalagmites from Paturau and Punakaiki limestone areas (New Zealand; Williams et al., 2004); black dashed line = T8 stalagmite of Cold Air Cave (South Africa; Holmgren et al., 2003); and (d) blue = VOSTOK ice core δD record (Dansgaard et al., 1993; Petit et al., 1999); red = $\delta^{18}\text{O}$ MD3 stalagmite, Nettlebed Cave (New Zealand; Hellstrom and McCulloch, 2000; Hellstrom et al., 1998); brown = $\delta^{18}\text{O}$ record of stalagmites from Paturau and Punakaiki limestone areas (New Zealand; Williams et al., 2004). YD = Younger Dryas; OD = Older Dryas

Zealand speleothem studies highlight the synchronism of the $\sim 15\text{ka}$ rapid transition with the BA transition observed in the Greenland. But, considering the fact that: (1) the analytical error at 2σ is variable: between 0.1 to 1 ka for the last 15 ka and sometimes reaching 1.8 at 20 ka (Hellstrom et al., 1998); (2) the interpolation of the 2σ age errors increases these errors (see MD3 growth curves envelopes, Fig. 5); (3) ice core chronology errors also increase significantly between 15 and 20 ka (where it is close to $\pm 2\text{ka}$; Schwander et al., 2001), efforts to improve N–S ice core chronologies are still topical (Blunier and Brook, 2001; Jouzel et al., 2001; Stocker and Johnsen, 2005). Consequently, there are no means to accurately detect any

leads and lags for these short climatic transitions at the moment.

On the T8 stalagmite of Cold Air Cave (South Africa), the beginning of the deglaciation is dated on the $\delta^{18}\text{O}$ record around 17–18 ka (Holmgren et al., 2003). But because of the slow growth rate during the lg period, dating precision is relatively poor (between 0.5 and 3 ka; Holmgren, 2002). In this relatively arid and warm area, the $\delta^{13}\text{C}$ is interpreted by the authors as a change in the relative proportion of C4 grasses: low values indicate sparse grass cover associated with dry conditions while high values are linked with a better grass cover; as a consequence, the $\delta^{13}\text{C}$ cannot be reasonably compared to our $\delta^{13}\text{C}$ record.

As a first conclusion, it appears that the Northern Hemisphere U–Th dated speleothem records (at least between $\sim 30^\circ\text{N}$ and $\sim 45^\circ\text{N}$: Villars, Chauvet, La Mine, Hulu and Dongge Caves) show a relatively rapid, synchronous, postglacial warming within $\sim \pm 0.5$ ka, between 15.5 and 16 ka, that is in agreement with the first sign of warming in the Greenland ice cores records (i.e. at the end of the H1 event), which is not the abrupt BA transition, which occurred later, ~ 14.5 ka ago (Groottes et al., 1993; NorthGRIPmembers, 2004) (Fig. 10). A common feature of all these North Hemisphere speleothem records is that the BA transition appears gradual up to the Allerød warm period (Figs. 8, 9). In the Southern Hemisphere, the timing of the first warming following the last glacial period seems to be earlier by ~ 3 ka ± 1.8 ka in New Zealand speleothems compared to the continuous North Hemisphere speleothems of La Mine Cave (Tunisia), Hulu Cave (China), but because of large age errors at this period where speleothem growth rate is low, this time offset must be considered with caution.

Comparison with marine records—Comparison with ^{14}C dated marine cores must be careful because of the variable reservoir effect (from 400 to 1500 yr) which could possibly increase the age errors (Siani et al., 2000; Waelbroeck et al., 2001). However, very similar features to our records are observed in several marine records from both the Northern and Southern Hemispheres. First, the $\delta^{18}\text{O}$ seawater and SST records of the Orca Basin, Gulf of Mexico (26.56°N) (Flower et al., 2004) shows the following: (1) the beginning of the warming occurred around 16 ka, significantly earlier than the abrupt Greenland BA transition (Fig. 3 in Flower et al., 2004); and (2) the transition toward the BA is gradual until the abrupt onset of the YD. These authors have suggested that this tropical record warming preceded Greenland by ~ 2 ka, leading to the important conclusion that heat was retained in the tropics during the H1 event, and thus giving the Atlantic thermohaline circulation a major role. However, we show here that there is no significant difference between our northern records (Villars Cave is at 45.3°N) and this tropical one, neither in the chronology within the 2σ error margin, nor in the shape of the climatic variations. This implies the following: (1) the mid-latitudes in Western Europe and North Africa were also under the influence of the tropical heat store during the H1 event, which seems unlikely; or (2) the abrupt ~ 14.5 ka BA transition is possibly partly amplified by a local effect due to abrupt changes in the sources of the precipitation over Greenland or local atmospheric circulation effects (Landais et al., 2005; Masson-Delmotte et al., 2005a; Severinghaus et al., 2004; Wunsch, 2004), and consequently is more or less pronounced in the other records, depending on their link with the $\delta^{18}\text{O}$ sources and their localization.

Second, the south-eastern Atlantic marine core RC11-83 from South Africa (42°S ; Piotrowski et al., 2004) has shown that the global overturning circulation began between 16 and 17 ka, significantly earlier than the abrupt

Greenland 14.5 ka BA transition, but close to the beginning of the warming we observe in the North Hemisphere and New Zealand speleothems. Moreover it seems from the relatively continuous trend observed in the neodymium isotope profile of this record that changes in the thermohaline circulation were progressive and did not switch between distinct glacial and interglacial modes. The authors explained this by a possible progressive northward shift of the sea ice edge in response to the increase of the insolation. Such a mechanism could be responsible for a progressive temperature increase over most of the Northern Hemisphere, bringing a gradual increase in the soil microbial and vegetation activities as indicated by the $\delta^{13}\text{C}$ records of our stalagmites. The fact that the CH_4 changes observed in ice core records (Chappellaz et al., 1997, 1993) display a similar trend and shape to our records during this period may also be related to changes in both ecosystem primary production in wetlands (van Huissteden, 2004) and terrestrial ecosystems where it was recently found that plants emit methane (Keppler et al., 2006).

5.3. The Bolling–Allerød: trend and events

A unique feature of the stalagmites studied here is the gradual $\delta^{13}\text{C}$ change observed during the BA transition, and during the BA itself, until the abrupt cooling of the onset of the YD (Figs. 8 and 10). While the La Mine $\delta^{13}\text{C}$ decrease is very regular, a small plateau around 14 ka is observed on the Vil-stm11 stalagmite (Fig. 8). The Chauvet Cave stalagmite, Chau-stm6, is slightly different because the BA transition, which occurred 15160 ± 250 yrs ago, is more abrupt but still within the error margin of the start of the $\delta^{13}\text{C}$ change observed on the Villars sample (Fig. 8). However, the full transition is not recorded and it might have started earlier. After this transition, the Chauvet Cave $\delta^{13}\text{C}$ decreases fairly regularly until the YD, similar to the other two stalagmites. Thanks to the high resolution sampling on this stalagmite, several climatic events are observed on the two isotope profiles ($\delta^{13}\text{C}$ and $\delta^{18}\text{O}$ increase) which can be correlated with Greenland ice core events (Figs. 8, 10):

- (1) the first one, at ~ 15.1 ka, only visible on the Chau-stm6 $\delta^{18}\text{O}$ record, consists of a short excursion separating a first warming phase that occurred at the beginning of the BA transition; this cooling event could mark the limit of the Pre-Bølling warming observed in Greenland records and Santa Barbara Basin records (Groottes et al., 1993; Hendy et al., 2002), but, because the transition here is incomplete, this could also be another event of the transition; a similar pattern is found on the Hulu and Dongge Cave records (Fig. 8);
- (2) the second one, visible on both isotopes, shows an amplitude maximum at ~ 14.15 ka and coincides with the small $\delta^{13}\text{C}$ plateau observed on the Vil-stm11 sample. This well marked event is synchronous with the Older Dryas (OD) already observed in many archives

and dated around 14 ka B.P. (Grootes et al., 1993; Hendy et al., 2002; Hughen et al., 1998); note that the climatic deterioration of this event started about 0.3 ka earlier;

- (3) the third one, distinct on the $\delta^{13}\text{C}$ profile at ~ 13.8 ka by a 1.3‰ increase, is only recorded by a small increase in the $\delta^{18}\text{O}$ profile;
- (4) the fourth event consists of a smoother $\delta^{18}\text{O}$ increase between ~ 13.14 and 13.33 ka which could be attributed to the Intra-Allerød Cold Period (IACP; Fig. 11); it is recorded in the $\delta^{13}\text{C}$ by a step in the general warming trend.

It is impressive to see how well the Hulu and Dongge Cave $\delta^{18}\text{O}$ records match our $\delta^{13}\text{C}$ profiles, especially the Villars and La Mine records: the former display the same regular climate amelioration trend until the YD onset and the three main events observed in the Chau-stm6 stalagmite (possibly correlated with the Pre-Bølling warming, the OD

and the IACP) are visible as small $\delta^{18}\text{O}$ excursions, especially in the Hulu Cave record (Figs. 8 and 11).

If the BA climate wiggles observed in the stalagmites can be linked with the Greenland ice core $\delta^{18}\text{O}$ changes, the overall trend of this period is that the Allerød appears warmer than the Bølling in all the speleothem records while it is the opposite in the Greenland ice cores. Many other climatic records display such a feature at widespread latitudes. Among the best dated ones with high resolution are:

- (1) the Santa Barbara basin record ($34^{\circ}17'\text{N}$), where Planktonic foraminifera $\delta^{18}\text{O}$ (*N. Pachyderma* mostly) testify to warmer temperatures during the Allerød than during the Bølling and where the Older Dryas is clearly visible and dated, as in the Chau-stm6 stalagmite, at ~ 14 ka (Hendy et al., 2002);
- (2) the Cariaco Basin record (Venezuela, $10^{\circ}40'\text{N}$) where sediments (reflectance grey scale) and biomarkers show

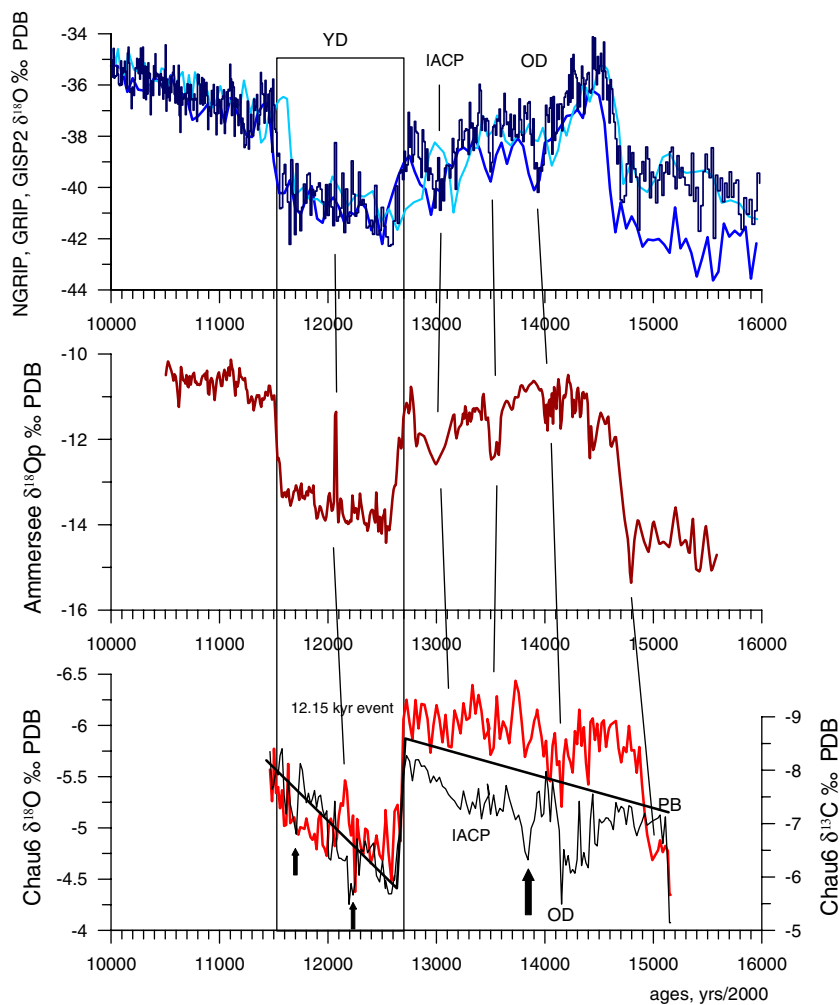


Fig. 11. Bølling-Allerød and Younger-Dryas climatic events from the Chau-stm6 stalagmite isotopic record (Chauvet Cave, S-France) (Bottom : red line = $\delta^{18}\text{O}$; black line = $\delta^{13}\text{C}$); comparison with: (1) (top) Greenland ice cores : NGRIP (blue; (NorthGRIPmembers, 2004), GRIP (dark blue; Dansgaard et al., 1993) and GISP2 (light blue; Grootes et al., 1993)); (2) Ammersee Lake $\delta^{18}\text{O}$ rainfall record from Ostracodes (Grafenstein Von et al., 1999). PB: Pre Bølling event; OD: Older Dryas; IACP: Inter Allerød Cold Period; 12.15 ka : warm event marked in the $\delta^{18}\text{O}$ records; (arrows) cold events marked in the Chau-stm6 $\delta^{13}\text{C}$ record. Thick black broken line: general climatic trend showing warming increases even during the YD.

- a relatively stable condition during the BA (Hughen et al., 2004; Hughen et al., 2000);
- (3) the Ammersee Lake $\delta^{18}\text{O}$ record (48°01'N; S-Germany) which displays a similar but less pronounced trend (Graffenstein Von et al., 1999); and
 - (4) the Monticchio Lake (40°56'N, South-Italy) pollen record, where the woody taxa display a gradual transition to the BA until the onset of the YD (Allen et al., 1999).

All these records suggest that, during the BA period, the temperature decreased in Greenland, while it remained stable or increased on the continent in Southern France and North-Africa, and possibly in several other places in the world. Thus, a pattern of a N–S gradient in the BA trend seems to occur, at least between Greenland, Ammersee and Chauvet Cave records (Fig. 11) which may be closely linked with the North-Atlantic ocean and atmospheric circulations and with sea ice cover extension.

5.3.1. The abrupt Younger–Dryas onset and the transition toward the Preboreal

The beginning of the YD is marked by an extremely rapid change in the $\delta^{13}\text{C}$ at 12700 ± 350 yr ago (error taken on the 2σ envelope; Fig. 5) for the Chauvet Cave stalagmite, 12900 ± 600 yr ago for the La Mine stalagmite and 12960 ± 580 yr ago for the Villars stalagmite, which is in agreement with Greenland ice core records 12880 ± 260 yr and with the Hulu Cave record 12823 ± 60 yr (Figs. 8, 10 and 11). The onset of the YD is not only synchronous (within the 2σ error margin) between these North Hemisphere records, but also very rapid in most records: the abrupt $\delta^{13}\text{C}$ increase observed in the Chauvet and La Mine samples occurred within about 75 and 80 yr, respectively (by linear age interpolation between U/Th dated points), in good agreement with the duration estimated in the Greenland records. The YD onset appears smoother on the Dongge cave record; it is nevertheless marked by a 0.6‰ $\delta^{18}\text{O}$ abrupt change at 12.7 ka (Dykoski et al., 2005). The Soreq Cave YD onset seems to have occurred earlier, at $\sim 13.4 \text{ ka} \pm \sim 0.2$, but the fact that between 11.9 and 15.6 ka, the record is constrained by only three dated points could explain this difference. An interesting feature is that the abruptness of the YD onset is followed, in the La Mine and Chauvet samples, by a relatively regular $\delta^{13}\text{C}$ decrease, suggesting a climatic improvement and vegetation development occurring immediately after the cooling, up to an optimum that was reached between 9500 and 10 000 yr ago (Figs 8, 11). This is also visible, in the Hulu Cave $\delta^{18}\text{O}$ record, and to a lesser extent, in the Greenland ice cores where the $\delta^{18}\text{O}$ increases by $\sim 2\text{‰}$ between 12.5 and 11.6 ka (Fig. 10). The abrupt transition toward the Pre-Boreal, ~ 11.6 – 1.4 ka, that is visible in the GRIP, NGRIP and GISP2 ice cores, is not observed in our samples which instead display a gradual transition, similar to the former BA transition (Figs 8, 10 and 11).

Consequently, it appears that the onset of the YD in Southern France and Northern Tunisia was so cold and/or dry at its beginning that the decline in vegetation and soil activity occurred within a few decades leading to drastic increase in the $\delta^{13}\text{C}$ signal. This is in agreement with pollen records from the Alboran Sea where the YD is well marked by a sudden increase in semi-desertic taxa (Combouret Nebout et al., 2002). The hypothesis of a dryer climate could explain the slower growth rate and hiatus in the Villars Cave sample during the YD, but an extremely cold climate that would have prevented water seepage by recurrent freezing is also a possibility. This can be explained by the proximity of the Villars Cave to the Atlantic Ocean: the cooling due to the cold marine streams of the North Atlantic circulation possibly controlled not only the atmospheric temperature but also the development of the vegetation and the seepage above the Villars Cave. But, for the Tunisian and the Chauvet Cave samples, a dryer climate is unlikely because the stalagmite growth rate curves do not show any substantial changes during this period (Fig. 5). There is no doubt that a part of the YD was wetter in some places : a sudden and strong increase precipitation in lake level from Switzerland, a few hundred kilometres east of the Chauvet Cave, has been observed (Magny and Bégeot, 2004); a south-western United States speleothem record shows a wetter climate soon after the onset of the YD possibly because of a more southern position of the North Hemisphere jet stream (Polyak and Güven, 2004). In a synthetic work about the last deglaciation, Walker (1995) notes that, in many northwest European records, there are indications of a climate amelioration during the last part of the YD (Walker, 1995). Not too far from our sites, a two fold division of the YD was recently observed in the Meerfeld Maar sediments, western Germany (Lucke and Brauer, 2004): a snowmelt discharge layer appears in the sediments suddenly after 12 240 varve years BP. This micro-facies change was interpreted as the possible consequence of higher winter (snow) precipitation. Such conditions, if they prevailed near the Chauvet Cave, could explain the unexpected high growth rate of the stalagmite during this period and also the observed $\delta^{18}\text{O}$ decrease. Consequently, it seems that there was a change in the rainfall pattern during the YD but regional differences modulated the speleothem records: the Villars Cave area was too dry or too cold during the YD to allow a continuous growth; this could be explained by its proximity to the Atlantic ocean but, on the other hand, the climate above the Chauvet and the La Mine Caves was likely to be as humid as the preceding Allerød period.

The debate over the existence of a YD in the Southern Hemisphere is still topical. Oscillations in the thermohaline circulation have been evoked in order to explain the apparent opposition between Southern and Northern temperature ice core records: the BA appears to be in phase with the Antarctic Cold Reversal and the YD with the second Antarctic warming. However, this N–phase

opposition is not certain. Firstly, (Bard et al., 1997) found synchronism in the Alkenone temperature reconstructions of 20°N and 20°S marine cores: the abrupt warming started at 15100 yr BP in phase with the GRIP record (14900 yr BP). Secondly, when examining the Dome Concordia ice core record EPICA it appears that the ACR has a similar timing and similar decreasing trend (the cooling after 14 ka) than that observed in the BA period recorded in the GRIP ice core record, the only difference resides in the later warming, which appears earlier in the Southern records while the YD is still visible in the Northern records (Stenni et al., 2001).

From the New Zealand speleothem records, the isotope cold reversals observed between 13.8 and 11.7 ka on stalagmites from the Nettlebed and Exhaleair Caves (Hellstrom and McCulloch, 2000), and between 13.5 and 11.1 ka, on the stalagmites from the Paturau and Punakaiki coastal limestone areas (Williams et al., 2004), span the Northern Hemisphere YD. But the timing, the length, and the typical shape characterised in the northern records by the abrupt onset, are different in these samples. The New Zealand Late Glacial Reversal (NZLGR) (Williams et al., 2004) which occurred between 13.53 and 11.14 ka in the New Zealand coastal stalagmite record, started earlier than the YD by about 0.83 ka but continued later by about 0.36 ka (values from Williams et al., 2004). Because the NZLGR has a similar timing to the Southern Hemisphere marine core reversal of the Great Australian Bight (32–4°S) (Andres et al., 2003) and to the glacial advance in South America (Hulton et al., 2002), it could be a specific cold event of the Southern Hemisphere, close to the ACR (Jouzel et al., 1993), but slightly delayed (Williams et al., 2004).

On the South Africa T8 stalagmite, the YD coincides with a hiatus which suggests that the YD cooling significantly influenced the climate at this 21°S latitude. The fact that the climate at this location is mainly under the influence of the southern Indian Ocean moisture, far from the north Atlantic freshwater discharges, suggests that a strong atmospheric link occurred during this period that was also shown by the Hulu Cave record.

However, as explained before, it seems to us that if we consider all the dating errors: the 2σ analytical, the interpolation between dated points for the U–Th ages, and the age models for the ice cores, it is still difficult to assert any significant time difference between these Southern Hemisphere records.

5.3.2. The 12.2 ka event

On the Chauvet Cave stalagmite, the middle of the YD is marked by a short $\delta^{18}\text{O}$ decrease event with a maximum at ~12150 yr ago and amplitude of almost -0.7% . From the $\delta^{18}\text{O}$ interpretation of the Chau-stm6 sample, this would be a warm event whose amplitude was almost half that of the YD onset. A similar event has already been noted by von Grafentsein in the $\delta^{18}\text{O}$ record of the Ammersee Lake record (Fig. 11) (Grafenstein Von et al., 1999), and

interpreted as a short, but distinct climatic event that left its imprint on the isotopic composition of the rainfall. It is also visible in the GRIP ice core where a short 2% $\delta^{18}\text{O}$ increase occurred at 12.2 ka (Fig. 11). A small $\delta^{18}\text{O}$ event can be seen on the La Mine stalagmite at the same time, but it is not visible in the Villars sample, probably due to the lower sampling resolution or to the rainfall $\delta^{18}\text{O}$ signal being obscured by isotopic fractionation during calcite precipitation. The sudden changes observed in the Meerfeld Maar that appeared precisely at 12240 varves years BP (Lucke and Brauer, 2004) coincides with the $\delta^{18}\text{O}$ decrease event observed in the Chauvet Cave. Although the sudden sedimentation change in this record might be due to a morphological and hydrological threshold, it might have been triggered by an unusual climatic event.

The middle YD event does not appear clearly in other records, however, it seems to have been recorded in the high resolution Santa Barbara basin core by a short 0.4% $\delta^{18}\text{O}$ increase in the *N. Pachyderma* record at ~12.3 ka (Fig. 4 in Hendy et al., 2002). It is not visible in the Cariaco basin palaeoclimate records, but there is a slight $\delta^{14}\text{C}$ excursion clearly visible in the middle of the YD (Fig. 4 in Hughen et al., 2000) that could be correlated with this event. In this case it could be linked with a change in the oceanic circulation or in solar activity, but more evidence is needed in order to understand it. Slightly before the 12.15 ka Chauvet $\delta^{18}\text{O}$ peak, the $\delta^{13}\text{C}$ record shows an increase at ~12190 yr suggesting, as in the $\delta^{13}\text{C}$ excursion observed during the BA, that a cold period occurred just before the warm one (Fig. 8). It is followed by a decrease of almost -2% , which occurred slightly after the $\delta^{18}\text{O}$ peak.

5.3.3. The ~9.3 ka event

Another remarkable event is visible at the climatic optimum of the beginning of the Holocene (Figs. 8, 11). It is marked, in Tunisia, by a $\sim 1\%$ $\delta^{13}\text{C}$ increase in the Min-stm1 stalagmite between 9.5 and 9.6 ± 0.65 ka and, in Southern China, by a $\sim 1.4\%$ $\delta^{18}\text{O}$ increase between 9.2 and $9.4 \pm \sim 0.15$ ka. This event could be correlated with a small negative $\delta^{18}\text{O}$ excursion in the NGRIP record at about 9.2 ka (Masson-Delmotte et al., 2005b) and coincides with a deposition hiatus in the Villars record that occurred between 9.9 and 8.7 ka (Figs. 8, 10). The fact that the Vil-stm11 sample stopped during this period could be the consequence of a fresh water discharge in the North Atlantic that modified drastically the environment around the Villars Cave, which is the site closest to the ocean, in a similar way to what happened during the YD, but other causes might also be considered. Right after this event, between ~8.0 and ~8.7 ka, stalagmite growth rates are maximum for the Dongge Cave sample, where it increases by a factor of 10, and also in the Villars sample where it reached 0.8 mm/yr as shown by the visible lamina. The fact that the known 8.2 ka event is not recorded in our stalagmites raises questions about its strength in the studied areas and also about its duration;

effectively, a few decades long event might have been missed in our record, especially if it is recorded by a growth hiatus.

6. Conclusion

The isotopic carbon signal of three stalagmites from Southern France and Northern Tunisia recorded the last deglaciation: the $\delta^{13}\text{C}$ variations are attributed to changes in soil and vegetation activity induced by temperature and humidity changes; the rapid response to well known climatic changes like the YD; the good synchronicity between the three $\delta^{13}\text{C}$ records; and the agreement with other records like the Chinese Cave $\delta^{18}\text{O}$ records demonstrate the relevance of the $\delta^{13}\text{C}$ signal as a global mid-latitude palaeoclimatic signal.

From the $\delta^{13}\text{C}$ profiles of the three studied stalagmites, we reconstructed the following Last Deglaciation climate events:

- o the BA transition started synchronously in all our samples from Southern France and Northern Tunisia between 15.5 and 16 ka; it is synchronous, within error margin ~ 0.5 ka, with the Hulu Cave record (China) and also with well dated marine and lake records from the Atlantic and Europe;
- o despite the global resemblance with the Greenland records, our speleothem records display marked differences with the ice core records: (1) the BA transition is gradual and only the incomplete Chauvet Cave stalagmite record displays an abrupt BA transition as in Greenland, but in this case, the transition is not completely recorded; (2) in all our records, the Allerød is warmer than the Bølling, which is also the case for several other well dated palaeoclimatic archives;
- o the YD onset is synchronous in all our records and occurred between 12.7 and 12.9 ± 0.5 ka; the cooling is extremely abrupt (i.e. ~ 70 – 80 years) and synchronous with the Chinese caves and Greenland ice core records; as soon as the YD onset occurs, a climatic amelioration trend appears, and similar to the BA transition, the Preboreal transition is gradual until an optimum at 9.5–10 ka is reached;
- o during the YD, the climate was so cold at the Villars Cave, that the growth rate slowed down drastically, likely due to the strong influence of the North Atlantic ocean circulation on this site. In the more continental Chauvet site, the stalagmite growth was as fast as the previous warm Allerød period, demonstrating that the YD was humid in this Southern part of the French Massif-Central, but not cold enough to prevent seepage; the same is observed, although less clearly, in the Northern Tunisia sample;
- o an abrupt event is recorded in the Tunisian and in the Villars records during the climatic optimum of the beginning of the Holocene at ~ 9.5 ka; it is synchronous, within error margin, with a well marked

event recorded in the Dongge cave stalagmite, S-China;

The $\delta^{13}\text{C}$ and $\delta^{18}\text{O}$ high resolution isotopic profiles of the Chau-stm6 stalagmite from the Chauvet Cave identify several climatic events: (1) cold events during the BA: at ~ 14 ka (possibly the OD) and at ~ 13.3 ka (possibly the IACP); (2) a warm event in the middle of the YD at ~ 12.15 ka which was also observed in the Ammersee Lake and in the Greenland $\delta^{18}\text{O}$ records, and which seems to be preceded by a few years by a cold event at about ~ 12.19 ka.

The comparison with the few Southern Hemisphere speleothem records available, also dated with U–Th TIMS methods, is still difficult because of large dating errors that occur where the growth rate is low; it seems to indicate that the first warming following the full glacial period seems to have occurred $\sim 3 \pm 1.8$ ka earlier in the New Zealand speleothems at a latitude close to the Villars and Chauvet Caves, but in the Southern Hemisphere. A more pronounced warming, clearly visible on the $\delta^{13}\text{C}$ isotope profile and on the growth curve of one stalagmite from New Zealand, appears at $\sim 16.7 \pm 0.5$ ka, slightly earlier than our NH samples. However, it is difficult to attribute any time leads or lags between the Southern Hemisphere cold reversals observed on the NZ speleothems with the north-YD cold period, principally because of the uncertainties in the U–Th ages of the transitions due to the 2σ analytical errors and the interpolation between dated points.

A simple explanation for the $\delta^{13}\text{C}$ deglaciation features observed in our stalagmite records can be proposed: the gradual increase of the 65°N insolation due to orbital changes moved the sea ice edge continuously northward since ~ 20 ka (as suggested by Piotrowski et al., 2004; Fig. 10) leading to a progressive temperature increase over the continents. During this “baseline temperature increase”, several events possibly due to greater or lesser discharges of the North American continental lakes (Donnelly et al., 2005) and to the Scandinavian ice sheet too, punctuated this “baseline” by cold events: OD, IACP, YD, and eventually the middle YD and the 9.3 ka events. But, what our continental records suggest is that the temperature continued to increase right after each of these events, which explains the warming trends clearly visible during the BA and YD (Fig. 11). The opposite Greenland $\delta^{18}\text{O}$ trend (i.e. during the BA and YD) could thus be explained by the fact that the ice $\delta^{18}\text{O}$ over Greenland was controlled not only by the local temperature but possibly also by a changes in the source $\delta^{18}\text{O}$ due to these large fresh water discharges of lower $\delta^{18}\text{O}$ values (Mazaud et al., 2000; Werner et al., 2001, 2000). The fact that the Hulu Cave $\delta^{18}\text{O}$ did not follow the Greenland $\delta^{18}\text{O}$ trend changes during the BA, and that it is so similar to the $\delta^{13}\text{C}$ signal of our samples, can then easily be explained by the fact that the large part of the rainfall sources of Hulu Cave are much too far from the Atlantic discharge area.

Acknowledgements

This work was funded by the CNRS and the CEA through different programs (ECLIPSE, PICS, PNEDC). We thank H. Versaveau, the Villars Cave owner, J. Clottes and J.M. Geneste for their help in the Chauvet Cave study and Th. Baritaud for his help in sampling. We are grateful to the GEOTOP (UQAM, Montreal, Canada) for its support during the writing of this article and to the following people for the availability of their data M. Bar-Matthews, K. Holmgren and P. Williams. Water stable isotopes from Villars and Chauvet sites were made by S. Falourd, O. Cattani and M. Stievenard, LSCE. The manuscript was improved thanks to the reviewers' comments especially S. Frisia's and thanks to fruitful discussions with U. von Grafenstein and V. Masson, LSCE.

Appendix A. Supplementary data

The online version of this article contains additional supplementary data. Please visit [doi:10.1016/j.quascirev.2005.01.030](https://doi.org/10.1016/j.quascirev.2005.01.030).

References

- Allen, J.R.M., Brandt, U., Brauer, A., Hubberten, H.-W., Huntley, B., Keller, J., Kraml, M., Mackensen, A., Mingram, J., Negendank, J.F.W., Nowaczyk, N.R., Oberhänsli, H., Watts, W.A., Wulf, S., Zolitschka, B., 1999. Rapid environmental changes in southern Europe during the last glacial period. *Nature* 400, 740–743.
- Alley, R.B., Meese, D.A., Shuman, C.A., Gow, A.J., Taylor, K.C., Grootes, P.M., White, J.W.C., Ram, M., Waddington, E.D., Mayewski, P.A., Zielinski, G.A., 1993. Abrupt increase in snow accumulation at the end of the Younger-Dryas event. *Nature* 362, 527–529.
- Andres, M.S., Bernosconi, S.M., McKenzie, J.A., Röhl, U., 2003. Southern Ocean deglacial record support global Younger Dryas. *Earth and Planetary Science Letters* 216, 515–524.
- Baker, A., Genty, D., Dreybrodt, W., Barnes, W.L., Mockler, N.J., Grapes, J., 1998. Testing theoretically predicted stalagmite growth rate with Recent annually laminated samples: implications for past stalagmite deposition. *Geochimica et Cosmochimica Acta* 62, 393–404.
- Baker, A., Ito, E., Smart, P.L., McEwan, R.F., 1997. Elevated and variable values of ^{13}C in speleothems in a British cave system. *Chemical Geology*, 263–270.
- Baker, A., Smart, P.L., Ford, D.C., 1993. Northwest European palaeoclimate as indicated by growth frequency variations of secondary calcite deposits. *Palaeogeography, Palaeoclimatology, Palaeoecology* 100, 291–301.
- Bar-Matthews, M., Ayalon, A., 2002. Climate reconstruction from Speleothems in the Eastern Mediterranean region. In: First ESF-HOLLVAR Workshop, Combining Climate Proxies. Lammi Biological Station, Finland, April 17–20th, 2002.
- Bar-Matthews, M., Ayalon, A., Gilmour, M., Matthews, A., Hawkesworth, C.J., 2003a. Sea-land oxygen isotopic relationships from planktonic foraminifera and speleothems in the Eastern Mediterranean region and their implication for paleorainfall during interglacial intervals. *Geochimica Et Cosmochimica Acta* 67, 3181–3199.
- Bar-Matthews, M., Ayalon, A., Kaufman, A., 1997. Late Quaternary paleoclimate in the eastern Mediterranean region from stable isotope analysis of speleothems at Soreq Cave, Israel. *Quaternary Research* 47, 155–168.
- Bar-Matthews, M., Ayalon, A., Kaufman, A., 2000. Timing and hydrological conditions of Sapropel events in the eastern Mediterranean, as evident from speleothems, Soreq cave, Israel. *Chemical Geology* 169, 145–156.
- Bar-Matthews, M., Ayalon, A., Kaufman, A., Wasserburg, G.J., 1999. The Eastern Mediterranean paleoclimate as a reflection of regional events: Soreq cave, Israel. *Earth and Planetary Science Letters* 166, 85–95.
- Bar-Matthews, M., Ayalon, A., G., A., M., and Ch. J., H., 2003b. Sea-Land oxygen isotopic relation ships from planktonic foraminifera and speleothems in the Eastern Mediterranean region and their implication for paleorainfall during interglacial intervals. *Geochimica Cosmochimica Acta* 67, 3181–3199.
- Bard, E., Rostek, F., Sonzogni, C., 1997. Interhemispheric synchrony of the last deglaciation inferred from alkenone palaeothermometry. *Nature* 385, 707–710.
- Beaulieu de, J.L., Reille, M., 1992. Long Pleistocene pollen sequences from the Velay Plateau (Massif Central, France). *Veget. Hist. Archaeobot.* 1, 233–242.
- Berger, A., Loutre, M.F., 1991. Insolation values for the climate of the last 10 million years. *Quaternary Sciences Review* 10, 297–317.
- Blunier, T., Brook, E.J., 2001. Timing of Millennial-Scale Climate Change in Antarctica and Greenland During the Last Glacial Period. *Science* 291, 109–112.
- Blunier, T., Chappellaz, J., Schwander, J., Dällenbach, A., Stauffer, B., Stocker, T.F., Raynaud, D., Jouzel, J., Clausen, H.B., Hammer, C.U., Johnsen, S.J., 1998. Asynchrony of Antarctic and Greenland climate during the last glacial. *Nature* 394, 739–743.
- Bond, G.C., Kromer, B., Beer, J., Muscheler, R., Evans, M.N., Showers, W., Hoffmann, S., Lotti-Bond, R., Hajdas, I., Bonani, G., 2001. Persistent Solar Influence on North Atlantic Climate During the Holocene. *Science* 294, 2130–2136.
- Bourges, F., Mangin, A., d'Hulst, D., 2001. Carbon dioxide in karst cavity atmosphere dynamics: the example of the Aven d'Orgnac (Ardeche). *Comptes Rendus De L Academie Des Sciences Serie Ii Fascicule a-Sciences De La Terre Et Des Planetes* 333, 685–692.
- Causse, C., Vincent, J.-S., 1989. Th/U disequilibrium dating of Middle and Late Pleistocene wood and shells from Banks and Victoria islands, Arctic Canada. *Canadian Journal of Earth Sciences* 26, 2718–2723.
- Chappellaz, J., Blunier, T., Kints, S., Dällenbach, A., Barnola, J.-M., Schwander, J., Raynaud, D., Stauffer, B., 1997. Changes in the atmospheric CH_4 gradient between Greenland and Antarctica during the Holocene. *Journal of Geophysical Research* 102 (D13), 15987–15997.
- Chappellaz, J., Blunier, T., Raynaud, D., Barnola, J.M., Schwander, J., Stauffer, B., 1993. Synchronous Changes in Atmospheric CH_4 and Greenland Climate between 40-Kyr and 8-Kyr Bp. *Nature* 366, 443–445.
- Chauvet, J.M., Brunel-Deschamps, E., Hillaire, C., 1995. “La grotte Chauvet.” Seuil.
- Clark, I.D., Lauriol, B., 1992. Kinetic enrichment of stable isotopes in cryogenic calcite. *Chemical Geology* 102, 217–228.
- Clottes, J., Chauvet, J.M., Brunel-Deschamps, E., Hillaire, C., Daugas, J. P., Arnold, M., Cachier, H., Evin, J., Fortin, P., Oberlin, C., Tisnerat, N., Valladas, H., 1995. Les peintures paléolithiques de la Grotte Chauvet-Pont d'Arc à Vallon-Pont-d'Arc (Ardèche, France): datations directes et indirectes par la méthode du radiocarbonate. *Comptes Rendus de l'Académie des Sciences de Paris* 320, **Serie IIa**, 1133–1140.
- Combouret, N., Turon, J.L., Zhan, R., Capotondi, L., Londeix, L., Pahnke, K., 2002. Enhanced aridity and atmospheric high-pressure stability over the western Mediterranean during the North Atlantic cold event of the past 50 ky. *Geology* 30, 863–866.
- Dansgaard, W., Johnsen, S.J., Clausen, H.B., Dahl-Jensen, D., Gundestrup, N.S., Hammer, C.U., Hvidberg, C.S., Steffensen, J.P., Sveinbjörnsdóttir, A.E., Jouzel, J., Bond, G., 1993. Evidence for general instability of past climate from a 250-yr ice-core record. *Nature* 364, 218–220.

- Delannoy, J.J., Debard, E., Ferrier, C., Kervazo, B., Perrette, Y., 2001. Contribution de la cartographie morphologique souterraine dans l'étude spéléogénique de la grotte Chauvet. Premiers éléments spéléogéniques et implications paléogéographiques, préhistoriques et paléontologiques. *Quaternaire* 12, 235–248.
- Denniston, R.F., Gonzalez, L.A., Asmerom, Y., Polyak, V., Ragan, M.K., Saltzman, M.R., 2001. A high-resolution speleothem record of climatic variability at the Allerod-Younger Dryas transition in Missouri, central United States. *Palaeogeography Palaeoclimatology Palaeoecology* 176, 147–155.
- Donnelly, J.P., Driscoll, N.W., Uchupi, E., Keigwin, L.D., Schwab, W.C., Thieler, E.R., Swift, S.A., 2005. Catastrophic meltwater discharge down the Hudson Valley: A potential trigger for the Intra-Allerod cold period. *Geology* 33, 89–92.
- Dorale, J.A., Edwards, R.L., Ito, E., Gonzales, L.A., 1998. Climate and vegetation history of the Midcontinent from 75 to 25 ka: A speleothem record from Crevice Cave, Missouri, USA. *Science* 282, 1871–1874.
- Dorale, J.A., Gonzales, L.A., Reagan, M.K., Pickett, D.A., Murrell, M.T., Baker, R.G., 1992. A high-resolution record of Holocene climate change in speleothem calcite from Cold Water Cave, Northeast Iowa. *Science* 258, 1626–1630.
- Drake, J.J., 1983. The effect of geomorphology and seasonality on the chemistry of carbonate groundwater. *Journal of Hydrology* 61, 223–236.
- Drysdale, R.N., Zanchetta, G., Hellstrom, J.C., Fallick, A.E., Zhao, J., Isola, I., Bruschi, G., 2004. Palaeoclimatic implications of the growth history and stable isotope (d18O and d13C) geochemistry of a Middle to Late Pleistocene stalagmite from central-western Italy. *Earth and Planetary Science Letters* 227, 215–229.
- Dulinski, M., Rozanski, K., 1990. Formation of 13C/12C isotope ratios in speleothems: a semi-dynamic model. *Radiocarbon* 32, 7–16.
- Dykoski, C.A., Edwards, R.L., Cheng, H., Yuan, D., Cai, Y., Zhang, M., Lin, Y., Qing, J., An, Z.S., Revenaugh, J., 2005. A high-resolution, absolute-dated Holocene and deglacial Asian monsoon record from Dongge Cave, China. *Earth and Planetary Science Letters* 233, 71–86.
- Edwards, R.L., Chen, J.H., Wasserburg, G.J., 1987. ^{238}U – ^{234}U – ^{230}Th – ^{232}Th systematics and the precise measurement of time over the past 500,000 years. *Earth and Planetary Science Letters* 81, 175–192.
- EPICA, m., 2004. Eight glacial cycles from an Antarctic ice core. *Nature* 429, 623–628.
- Fantidis, J., Ehhalt, D.H., 1970. Variations of the carbon and oxygen isotopic composition in stalagmites and stalactites: evidence of non-equilibrium isotopic fractionation. *Earth and Planetary Science Letters* 10, 136–144.
- Flower, B.P., Hastings, D.W., Hill, H.W., Quinn, T.M., 2004. Phasing of deglacial warming and Laurentide Ice Sheet meltwater in the Gulf of Mexico. *Geology* 32, 597–600.
- Ford, D.C., Williams, P., 1992. *Karst Geomorphology and Hydrology*. Chapman & Hall.
- Fornaci-Rinaldi, G., Panichi, C., Tongiorgi, E., 1968. Some causes of the variation of the isotopic composition of carbon and oxygen in cave concretions. *Earth and Planetary Science Letters* 4, 321–324.
- Frisia, S., Borsato, A., Spötl, C., Villa, I. M., Cucchi, F., 2005. Climate Variability in the South-Eastern Alps of Italy over the last 17000 years. *Boreas* 34.
- Ganopolski, A., Rahmstorf, S., 2002. Abrupt glacial climate changes due to stochastic resonance. *Physical Review Letters* 88, 038501-1–038501-4.
- Gasse, F., 2000. Hydrological changes in the African tropics since the Last Glacial Maximum. *Quaternary Science Reviews* 19, 189–211.
- Genty, D., Baker, A., Massault, M., Proctor, C., Gilmour, M., Pons-Branchu, E., Hamelin, B., 2001a. Dead carbon in stalagmites: Carbonate bedrock paleodissolution vs. ageing of soil organic matter. Implication for 13C variation in speleothems. *Geochimica et Cosmochimica Acta* 65, 3443–3457.
- Genty, D., Baker, A., Vokal, B., 2001b. Intra- and inter-annual growth rate of modern stalagmites. *Chemical Geology* 176, 191–212.
- Genty, D., Blamart, D., Ghaleb, B., Plagnes, V., Causse, C., Bakalowicz, M., Melière, M.A., Zouari, K., Chkir, N., 2004a. The Last deglaciation recorded in the d13C of stalagmites from South-France and Tunisia. International Workshop on the Application of Isotope Techniques in Hydrological and Environmental Studies, Paris, France.
- Genty, D., Blamart, D., Ouahdi, R., Gilmour, M., Baker, A., Jouzel, J., Van-Exter, S., 2003. Precise dating of Dansgaard-Oeschger climate oscillations in western Europe from stalagmite data. *Nature* 421, 833–837.
- Genty, D., Deflandre, G., Quinif, Y., Verheyden, S., 1997. Les lamines de croissance des spéléothèmes: origine et intérêt paléoclimatique. *Bulletin de la Société belge de Géologie* 106, 63–77.
- Genty, D., Ghaleb, B., Plagnes, V., Causse, C., Valladas, H., Blamart, D., Massault, M., Geneste, J.M., Clottes, J., 2004b. Datations U/Th (TIMS) et 14C (AMS) des stalagmites de la grotte Chauvet (Ardeche, France): intérêt pour la chronologie des événements naturels et anthropiques de la grotte. *Comptes Rendus PLEVOL* 3, 629–642.
- Genty, D., Massault, M., 1999. Carbon transfer dynamics from bomb- ^{14}C and $\delta^{13}\text{C}$ time series of a laminated stalagmite from SW France—modelling and comparison with other stalagmite records. *Geochimica et Cosmochimica Acta* 63, 1537–1548.
- Goslar, T., Wohlfarth, B., Possnert, G., Björck, J., 1999. Variations of atmospheric ^{14}C concentration over the Allerod-Younger Dryas transition. *Climate Dynamics* 15, 29–42.
- Grafenstein Von, U., Erlenkeuser, H., Brauer, A., Jouzel, J., Johnsen, J., 1999. A Mid-European Decadal Isotope-Climat Record from 15,500 to 5000 years B.P. *Science* 284, 1654–1657.
- Grootes, P.M., Stuiver, M., White, J.W.C., Johnsen, S., Jouzel, J., 1993. Comparison of oxygen isotope records from the GISP2 and GRIP Greenland ice cores. *Nature* 366, 552–554.
- Guiot, J., de Beaulieu, J.L., Cheddadi, R., David, F., Ponel, P., Reille, M., 1993. The climate in Western Europe during the last Glacial/Interglacial cycle derived from pollen and insect remains. *Palaeogeography, Palaeoclimatology, Palaeoecology* 103, 73–93.
- Hellstrom, J., McCulloch, M., 2000. Multi-proxy constraints on the climatic significance of trace element records from a New-Zealand speleothem. *Earth and Planetary Science Letters* 179, 287–297.
- Hellstrom, J., McCulloch, M., Stone, J., 1998. A detailed 31,000-year record of climate and vegetation change, from the isotope geochemistry of two New Zealand speleothems. *Quaternary Research* 50, 167–178.
- Hendy, C.H., 1971. The isotopic geochemistry of speleothems—I. The calculation of the effects of different modes of formation on the isotopic composition of speleothems and their applicability as palaeoclimatic indicators. *Geochimica et Cosmochimica Acta* 35, 801–824.
- Hendy, I.L., Kennett, J.P., Roark, E.B., Ingram, B.L., 2002. Apparent synchronicity of submillennial scale climate events between Greenland and Santa Barbara Basin, California from 30–10 ka. *Quaternary Science Reviews* 21, 1167–1184.
- Holmgren, K., 2002. Climate reconstruction from speleothems in South Africa. In “First ESF-HOLLVAR workshop, Combining climate proxies.” Lammi Biological Station, Finland, April 17–20th 2002.
- Holmgren, K., Lee-Thorp, J.A., Cooper, G.R., Lundblad, K., Partridge, T.C., Scott, L., Sitaldeen, R., Talma, A.S., Tyson, P.D., 2003. Persistent millennial-scale climatic variability over the past 25,000 years in Southern Africa. *Quaternary Science Reviews* 22, 2311–2326.
- Hughen, K.A., Eglinton, T.I., Li, X., Makou, M., 1995. Abrupt tropical vegetation response to rapid climate changes. *Science* 304, 1955–1959.
- Hughen, K.A., Eglinton, T.I., Li, X., Makou, M., 2004. Abrupt tropical vegetation response to rapid climatic changes. *Science* 304, 1955–1959.
- Hughen, K.A., Overpeck, J.T., Lehman, S.J., Kashgarian, M., Southon, J., Peterson, L.C., Alley, R., Sigma, D.M., 1998. Deglacial changes in ocean circulation from an extended radiocarbon calibration. *Nature* 391, 65–68.
- Hughen, K.A., Southon, J.R., Lehman, S.J., Overpeck, J.T., 2000. Synchronous Radiocarbon and Climate Shifts During the Last Deglaciation. *Science* 290, 1951–1954.

- Hulton, N.R.J., Purves, R.S., McCulloch, R.D., Sughen, D.E., Bentley, M.J., 2002. The Last Glacial Maximum and deglaciation in southern South America. *Quaternary Science Reviews* 21, 233–241.
- Jouzel, J., Barkov, N.I., Barnola, J.-M., Bender, M., Chappellaz, J., Genthon, C., Kotlyakov, V.M., Lipenkov, V., Lorius, C., Petit, J.R., Raynaud, D., Raisbeck, G., Ritz, C., Sowers, T., Stievenard, M., Yiou, F., Yiou, P., 1993. Extending the Vostok ice-core record of palaeoclimate to the penultimate glacial period. *Nature* 364, 407–412.
- Jouzel, J., Masson, V., Cattani, O., Falourd, S., Stievenard, M., Stenni, B., Longinelli, A., Johnsen, S.J., Steffensen, J.P., Petit, J.R., Schwander, J., Souchez, R., Barkov, N.I., 2001. A new 27ky high resolution East Antarctic climate record. *Geophysical Research Letters* 28, 3199–3202.
- Kendall, A.C., Broughton, P.L., 1978. Origin of fabrics in speleothems composed of columnar calcite crystals. *Journal of Sedimentary Petrology* 48, 519–538.
- Keppler, F., Hamilton, J.T.G., Brass, M., Rockmann, T., 2006. Methane emissions from terrestrial plants under aerobic conditions. *Nature* 439, 187–191.
- Kim, S.-T., O'Neil, J.R., 1997. Equilibrium and nonequilibrium oxygen isotope effect in synthetic carbonates. *Geochimica et Cosmochimica Acta* 61, 3461–3475.
- Landais, A., Jouzel, J., Masson-Delmotte, V., Caillon, N., 2005. Large temperature variations over rapid climatic events in Greenland: a method based on air isotopic measurements. *Comptes Rendus Geoscience* 337, 947–956.
- Liu, Z.H., Dreybrodt, W., 1997. Dissolution kinetics of calcium carbonate minerals in H₂O–CO₂ solutions in turbulent flow: The role of the diffusion boundary layer and the slow reaction H₂O+CO₂ reversible arrow H⁺+HCO³⁻. *Geochimica Et Cosmochimica Acta* 61, 2879–2889.
- Lucke, A., Brauer, A., 2004. Biogeochemical and micro-facial fingerprints of ecosystem response to rapid Late Glacial climatic changes in varved sediments of Meerfelder Maar (Germany). *Palaeogeography Palaeoclimatology Palaeoecology* 211, 139–155.
- Ludwig, K.R., 2003. *Isoplot 3.0*. Berkeley Geochronology Center Special Publication, vol. 4.
- Magny, M., Bégeot, C., 2004. Hydrological changes in the European midlatitudes associated with freshwater outbursts from Lake Agassiz during the Younger Dryas event and the early Holocene. *Quaternary Research* 61, 181–192.
- Magri, D., Sadori, L., 1999. Late Pleistocene and Holocene pollen stratigraphy at Lago di Vico, central Italy. *Vegetation History and Archaeobotany* 8, 247–260.
- Masson-Delmotte, V., Jouzel, J., Landais, A., Stievenard, M., Johnsen, S.J., White, J.W.C., Werner, M., Sveinbjornsdottir, A., Fuhrer, K., 2005a. GRIP deuterium excess reveals rapid and orbital-scale changes in Greenland moisture origin. *Science* 309, 118–121.
- Masson-Delmotte, V., Landais, A., Stievenard, M., Cattani, O., Falourd, S., Jouzel, J., Johnsen, S.J., Jensen, D.D., Sveinbjornsdottir, A., White, J.W.C., Popp, T., Fischer, H., 2005b. Holocene climatic changes in Greenland: different deuterium excess signals at Greenland Ice Core Project (GRIP) and NorthGRIP. *Journal of Geophysical Research-Atmospheres* 110.
- Mazaud, A., Vimeux, F., Jouzel, J., 2000. Short fluctuations in Antarctic isotope records: a link with cold event in the North Atlantic? *Earth and Planetary Science Letters* 177, 219–225.
- McDermott, F., 2004. Paleo-climate reconstruction from stable isotope variations in speleothems: a review. *Quaternary Science Reviews* 23, 901–918.
- Mickler, P.J., Banner, J.L., Stern, L., Asmerom, Y., Edwards, R.L., Ito, E., 2004. Stable isotope variations in modern tropical speleothems: evaluating equilibrium vs. kinetic isotope effects. *Geochimica Et Cosmochimica Acta* 68, 4381–4393.
- Nigemann, S., Mangini, A., Richter, D.K., Wurth, G., 2003. A paleoclimate record of the last 17,600 years in stalagmites from the B7 cave, Sauerland, Germany. *Quaternary Science Reviews* 22, 555–567.
- NorthGRIPmembers, 2004. High resolution climate record of the Northern hemisphere reaching into the Last Interglacial period. *Nature* 43, 147–151.
- O'Neil, J.R., Clayton, R.N., Mayeda, T.K., 1969. Oxygen isotope fractionation in divalent metal carbonates. *Journal of Chemical Physics* 51, 5547–5558.
- Paquereau, M.M., 1980. Chronologie palynologique du Pleistocene dans le Sud-Ouest de la France. *Supplément au Bulletin de l'AFEQ* 1, 298–306.
- Petit, J.R., Jouzel, J., Raynaud, D., Barkov, N.I., Barnola, J.-M., Basile, I., Benders, M., Chappellaz, J., Davis, M., Delaygue, G., Delmotte, M., Kotlyakov, V.M., Legrand, M., Lipenkov, V.Y., Lorius, C., Pépin, L., Ritz, C., Saltzman, E., Stievenard, M., 1999. Climate and atmospheric history of the past 420,000 years from the Vostok ice core, Antarctica. *Nature* 399, 429–436.
- Piotrowski, A.M., Goldstein, S.L., Hemming, S.R., Fairbanks, R.G., 2004. Intensification and variability of the ocean thermohaline circulation through the last deglaciation. *Earth and Planetary Science Letters* 225, 205–220.
- Polyak, V.J., Güven, N., 2004. Silicates in carbonate speleothems, Guadalupe mountains, New Mexico, USA. In: Sasowsky, I.D., Mylroie, J. (Eds.), *Studies of cave sediments—Physical and chemical records of paleoclimate*. Kluwer Academic, Plenum Publishers, New York.
- Rahmstorf, S., 2002. Ocean circulation and climate during the past 120,000 years. *Nature* 419, 207–214.
- Rahmstorf, S., 2003. The current climate. *Nature* 421, 699.
- Renssen, H., van Geel, B., van der Plicht, J., Magny, M., 2000. Reduced solar activity as a trigger for the start of the Younger Dryas? *Quaternary International* 68–71, 371–383.
- Rozanski, K., Araguas-Araguas, L., Gonfiantini, R., 1993. Isotopic patterns in modern global precipitation, in climate change in continental isotopic records. *Geophysical Monograph* 78, 1–36.
- Salomon, W., Mook, W.G., 1986. Isotope geochemistry of carbonates in the weathering zone, *Handbook of Environmental*. In: Fritz, P., Fontes, J.Ch. (Eds.), *Isotope Geochemistry*. pp. 239–269.
- Schwander, J., Jouzel, J., Hammer, C.U., Petit, J.-R., Udisti, R., Wolff, E., 2001. A tentative chronology for the EPICA Dome Concordia. *Geophysical Research Letters* 28, 4243–4246.
- Severinghaus, J., Jouzel, J., Caillon, N., Stocker, T.F., 2004. Comment on Greenland-Antarctic phase relations and millennial time-scale climate fluctuations in the Greenland ice-cores by C. Wunsh. *Quaternary Science Reviews* 23, 2053–2055.
- Siani, G., Paterne, M., Arnold, M., Bard, E., Métyvier, B., Tisnerat, N., Bassinot, F., 2000. Radiocarbon reservoir ages in the Mediterranean Sea and Black Sea. *Radiocarbon* 42, 271–280.
- Stager, J.C., Mayewski, P.A., Meeker, L.D., 2002. Cooling cycles, Heinrich event 1, and the desiccation of Lake Victoria. *Palaeogeography Palaeoclimatology Palaeoecology* 183, 169–178.
- Stenni, B., Masson-Delmotte, V., Johnsen, S., Jouzel, J., Longinelli, A., Monnin, E., Röthlisberger, Selmo, E., 2001. An oceanic cold reversal during the last deglaciation. *Science* 293, 2074–2077.
- Stocker, T.F., Johnsen, S.J., 2005. A minimum thermodynamic model for the bipolar seesaw (vol 18, pg 1087, 2003). *Paleoceanography* 20.
- Talma, A.S., Vogel, J.C., 1992. Late Quaternary paleotemperatures derived from a speleothem from Cango Caves, Cape Province, South Africa. *Quaternary Research* 37.
- Thompson, L.G., Mosleythompson, E., Davis, M.E., Lin, P.N., Henderson, K.A., Coledai, J., Bolzan, J.F., Liu, K.B., 1995. Late-glacial stage and holocene tropical ice core records from Huascarán, Peru. *Science* 269, 46–50.
- Thornthwaite, C.W., 1954. The Measurement of Potential Evapotranspiration.
- Turon, J.L., Lezine, A.M., Deneffe, M., 2003. Land-sea correlations for the last glaciation inferred from a pollen and dinocyst record from the Portuguese margin. *Quaternary Research* 59, 88–96.

- Valladas, H., Clottes, J., Geneste, J.M., Garcia, M.A., Arnold, M., Cachier, H., Tisnerat-Laborde, N., 2001. Evolution of prehistoric cave art. *Nature* 413, 479.
- van Geel, B., van der Plicht, J., Renssen, H., 2003. Major Delta C-14 excursions during the late glacial and early Holocene: changes in ocean ventilation or solar forcing of climate change? *Quaternary International* 105, 71–76.
- van Huissteden, J., 2004. Methane emission from northern wetlands in Europe during oxygen isotope stage 3. *Quaternary Science Reviews* 23, 1989–2005.
- Vogel, J.C., Kronfeld, J., 1997. Calibration of radiocarbon dates for the late Pleistocene using U/Th dates on stalagmites. *Radiocarbon* 39, 27–32.
- Waelbroeck, C., Duplessy, J.C., Michel, E., L., L., Paillard, D., Duprat, J., 2001. The timing of the last deglaciation in North Atlantic climate records. *Nature* 412, 724–727.
- Walker, M.J.C., 1995. Climatic changes in Europe during the last glacial/interglacial transition. *Quaternary International* 28, 63–76.
- Wang, Y.J., Cheng, H., Edwards, R.L., An, Z.S., Wu, J.Y., Shen, C.C., Dorale, J.A., 2001. A high-resolution absolute-dated late Pleistocene monsoon record from Hulu Cave, China. *Science* 294, 2345–2348.
- Werner, M., Heimann, M., Hoffman, G., 2001. Isotopic composition and origin of polar precipitation in present and glacial climate simulations. *Tellus Series B-Chemical and Physical Meteorology* 53, 53–71.
- Werner, M., Mikolajewicz, U., Hoffmann, G., Heimann, M., 2000. Possible changes of delta O-18 in precipitation caused by meltwater event in the North Atlantic. *Journal of Geophysical Research—Atmospheres* 105, 10161–10167.
- Williams, P.W., King, D.N.T., Zhao, J.-X., Collerson, K.D., 2004. Late Pleistocene to Holocene composite speleothem 18O and 13C chronologies from South Island, New-Zealand—did a global Younger Dryas really exist? *Earth and Planetary Science Letters* 230, 301–307.
- Wunsch, C., 2004. Quantitative estimate of the Milankovitch-forced contribution to observed Quaternary climate change. *Quaternary Science Reviews* 23, 1001–1012.
- Wurth, G., Niggeman, S., Richter, D.K., Mangini, A., 2004. The Younger Dryas and Holocene climate record of a stalagmite from the Hölloch Cave (Bavarian Alps, Germany). *Journal of Quaternary Science* 19, 291–298.
- Zhao, J.X., Wang, Y.J., Collerson, K.D., Gagan, M.K., 2003. Speleothem U-series dating of semi-synchronous climate oscillations during the last deglaciation. *Earth and Planetary Science Letters* 216, 155–161.
- Zolitschka, B., 1992. Climatic change evidence and lacustrine varves from maar lakes, Germany. *Climate Dynamics* 6, 229–232.